



**Michigan  
Technological  
University**

Michigan Technological University  
**Digital Commons @ Michigan Tech**

---

Dissertations, Master's Theses and Master's Reports

---

2018

# DESIGN OPTIMIZATION AND HIGH CYCLE FATIGUE ANALYSIS AND OF A DIFFERENTIAL CASE

Praveen Bulusu Surya Naga  
*Michigan Technological University*, [pbulusus@mtu.edu](mailto:pbulusus@mtu.edu)

Copyright 2018 Praveen Bulusu Surya Naga

---

## Recommended Citation

Bulusu Surya Naga, Praveen, "DESIGN OPTIMIZATION AND HIGH CYCLE FATIGUE ANALYSIS AND OF A DIFFERENTIAL CASE", Open Access Master's Report, Michigan Technological University, 2018.  
<https://digitalcommons.mtu.edu/etdr/652>

Follow this and additional works at: <https://digitalcommons.mtu.edu/etdr>



Part of the [Computer-Aided Engineering and Design Commons](#)

DESIGN OPTIMIZATION AND HIGH CYCLE FATIGUE ANALYSIS AND OF A  
DIFFERENTIAL CASE

By

Praveen Bulusu Surya Naga

A REPORT

Submitted in partial fulfillment of the requirements for the degree of

MASTER OF SCIENCE

In Mechanical Engineering

MICHIGAN TECHNOLOGICAL UNIVERSITY

2018

© 2018 Praveen Bulusu Surya Naga

This report has been approved in partial fulfillment of the requirements for the Degree of MASTER OF SCIENCE in Mechanical Engineering.

Department of Mechanical Engineering – Engineering Mechanics

Report Advisor: *Dr. Gregory Odegard*  
Committee Member: *Dr. Paul Sanders*  
Committee Member: Dr. Hassan Masoud  
Department Chair: *Dr. William Predebon*

# Contents

1	Introduction.....	1
1.1	Overview .....	1
1.2	Terminology .....	2
1.3	Objective and scope of work .....	2
1.3.1	Topology Optimization.....	2
1.3.2	Static Stress and Fatigue Analyses .....	3
1.4	Design Criteria .....	3
1.5	Material Model .....	3
1.6	Loading and Boundary Conditions.....	4
1.6.1	Loading .....	4
1.6.2	Contacts and Constraints.....	6
1.6.3	Boundary Conditions .....	6
2	Initial Analysis .....	8
2.1	Results .....	8
2.2	Mesh Quality .....	10
2.3	Mesh Convergence .....	11
2.3.1	Mesh convergence study results .....	12
3	Topology optimization.....	14
3.1	Theory .....	14
3.1.1	Definitions.....	14
3.1.2	Structural Optimization.....	15
3.2	Optimization method.....	15
3.2.1	Design variables.....	15
3.2.2	Responses.....	16
3.2.3	Optimization Constraints .....	18
3.2.4	Objective Function.....	18
3.3	Optimization Results .....	18
3.3.1	Geometry refinement .....	19
4	Re-Analysis.....	22
4.1	Results .....	22
4.2	Summary .....	26

5	Fatigue analysis.....	27
5.1	Surface Stress extraction .....	27
5.1.1	Need for Critical Plane Fatigue analysis.....	27
5.2	Ductile Iron S-N curve .....	30
5.3	Fatigue life prediction method .....	30
5.4	Results .....	33
5.5	Conclusions and Future work.....	34
6	Reference List .....	35

## List of figures

Figure 1: (a) Differential assembly (AAM 2018) (b) Case (Eaton 2016).....	1
Figure 2: Differential case regions.....	2
Figure 3: Ring gear loads - a) Reverse cases b) Forward cases c) Loads at 10 <sup>0</sup> interval.....	5
Figure 4 : Internal gear and bearing pre-loads .....	5
Figure 5 : Contacts and Constraints .....	6
Figure 6 : Boundary conditions.....	7
Figure 7 : Critical Locations – 1- von Mises stress plots.....	8
Figure 8 : Critical locations – 2 - von Mises stress plots .....	8
Figure 9 : Element sets at critical locations .....	9
Figure 10 : Max. von-Mises stress at all critical locations vs step number .....	9
Figure 11 : Mesh plot showing warning elements (yellow) .....	10
Figure 12: Zoomed mesh plots .....	11
Figure 13 : Stress and percent difference v. mesh size - Flange Fillet .....	12
Figure 14 : Stress and percent difference v. mesh size - Bearing Fillet.....	12
Figure 15 : Stress and percent difference v. mesh size - Big window fillet - 1 .....	12
Figure 16 : Stress and percent difference v. mesh size - Big window fillet - 2 .....	13
Figure 17 : Stress and percent difference v. mesh size - Internal fillet - 1 .....	13
Figure 18 : Stress and percent difference v. mesh size - Internal fillet – 2.....	13
Figure 19 : The volumes at flange and bell ends constitute the design space .....	16
Figure 20 : Critical regions for which local compliance response is defined.....	17
Figure 21: FEM settings - a) Compliance response regions (in white); b) DRESP 2/L card .....	17
Figure 22: a) Die pull out direction constraints b) Example of draw constrains from [4].	18

Figure 23 : Topology results - element density plots.....	19
Figure 24 : Geometry refinement process.....	19
Figure 25 : Parametrized geometry - flange end.....	20
Figure 26 : Parametrized geometry - bell end.....	20
Figure 27: Parametrized geometry - barrel region.....	20
Figure 28 : Max. Principal stress plots - internal fillet 1 .....	22
Figure 29: Max. Principal stress plots - internal fillet 2 .....	23
Figure 30: Max. Principal stress plots - internal fillet 3 .....	23
Figure 31: Max. Principal stress plots - Flange fillet.....	24
Figure 32: Max. Principal stress plots - Big window fillet 1 .....	24
Figure 33 : Max. Principal stress plots - Big window fillet 2 .....	25
Figure 34: Max. Principal stress plots - Window region .....	25
Figure 35: Max. Principal stress plots -Internal corner region .....	26
Figure 36 : Membrane elements on the surface .....	27
Figure 37: Uni-axial alternating stress example .....	28
Figure 38 : Several loading scenario examples.....	28
Figure 39 : a) Stress state history of a membrane element b) example of proportionally varying stresses .....	29
Figure 40 : Ductile iron S-N Curve [7].....	30
Figure 41: Fatigue fracture and critical plane normals .....	31
Figure 42 : Fatigue life prediction algorithm.....	32
Figure 43: Fatigue damage plot .....	33
Figure 44 : Fatigue life plots.....	34
Figure 45: Barrel region material removal.....	40





## List of tables

Table 1: Material Properties - DI 7003 .....	3
Table 2: Ring Gear Loads - at 5,875,000 N-mm .....	4
Table 3 : Internal Gear and Bearing preloads .....	4
Table 4 : Element quality criteria.....	10
Table 5: Mesh Statistics .....	11
Table 6 : Results Summary .....	26

## **Acknowledgements**

I thank Dr. Gregory Odegard and Dr. Paul Sanders for giving me an opportunity to work with the LIFT team and their support and guidance during this project. I also thank Mr. Russell Stein for his input.

I am grateful to my parents, my brother, my professors, mentors and friends for their support all throughout my life.

## **List of abbreviations**

AAM – American Axle and Manufacturing

CAD – Computer Aided Design

DOF – Degree of Freedom

FEM – Finite Element Method

FEA – Finite Element Analysis

FFP – Fatigue Fracture Plane

HCF – High Cycle Fatigue

LIFT – Lightweight Innovations for Tomorrow

MPC – Multi Point Constraint

SIMP – Solid Isotropic Material with Penalization

## Symbols

- $\alpha$  - Angle between fatigue fracture plane and critical plane
- $f_{-1}$  - Fatigue limit in fully reversed tensile test
- $t_{-1}$  - Fatigue limit in fully reversed tensile test
- $\beta$  - Critical damage value
- $\sigma_{a,c}$  - Alternating normal stress amplitude on the critical plane
- $\tau_{a,c}$  - Alternating shear stress amplitude on the critical plane
- $\sigma_{m,c}$  - Mean stress on the critical plane
- $\eta$  - Mean stress correction factor
- $f_{Nf}$  - Fatigue strength in fully reversed tensile test for  $N$  cycles
- $t_{Nf}$  - Fatigue strength in fully reversed shear test for  $N$  cycles
- $s$  - Ratio between the fatigue limits of fully reversed tensile and shear tests

## **Abstract**

Lightweight Innovations for Tomorrow (LIFT) is a consortium with several industries, universities and research institutes. It is operated by the American Lightweight Materials Manufacturing Innovation Institute (ALMMII). One of their projects, melt 5a, is to develop high silicon ductile iron (DI) alloys with improved mechanical properties and thin walled DI castings. These alloys have high strength to weight ratio compared to that of standard ductile iron (7003). Using these alloys, components can be re-designed that are much lighter which results in improved fuel efficiency, and reduced manufacturing costs and emissions.

In this project, a differential case is being re-designed with the objective of at least 25% weight reduction, while meeting strength requirements. The baseline design is obtained from Eaton, a power management company and a supplier of automotive differentials. The differential case is subjected to torsional, bending and gear thrust loads. With advancement in computational power and cutting-edge algorithms, methods such as topology optimization are being used to generate optimized designs. Using such method, a design that is 18.5% lighter than the original design with justifiable violations of the design criteria, is produced. Also, the design is analyzed for high cycle fatigue using a multi-axial critical plane approach to identify potential crack initiation sites.

# 1 Introduction

Stringent emission regulations and the need to reduce costs drive the development of lightweight vehicles. Reducing the total vehicle weight by 50 kg cuts down CO<sub>2</sub> emissions by 5g per km and increases fuel economy by 2% [1].

A differential case is an essential component of a vehicle's drivetrain. It acts as a structural member, transferring torque from the gearbox transmission to the axle shafts. It also acts as a carrier to internal gears, locking components, thrust washers and cross shaft. This component is being re-designed to reduce weight with the help of improved material properties. Finite Element Analysis (FEA) tools are used to analyze and investigate regions where material can be removed.

## 1.1 Overview

American Axle and Manufacturing (AAM) is a manufacturer of automotive drivetrain products. The 8.6 axle differential shown in Figure 1 is supplied by Eaton to AAM who provided the design criteria described in section 1.4. The improvement in mechanical properties of ductile iron is leveraged to re-design the differential case, a key component of the differential.

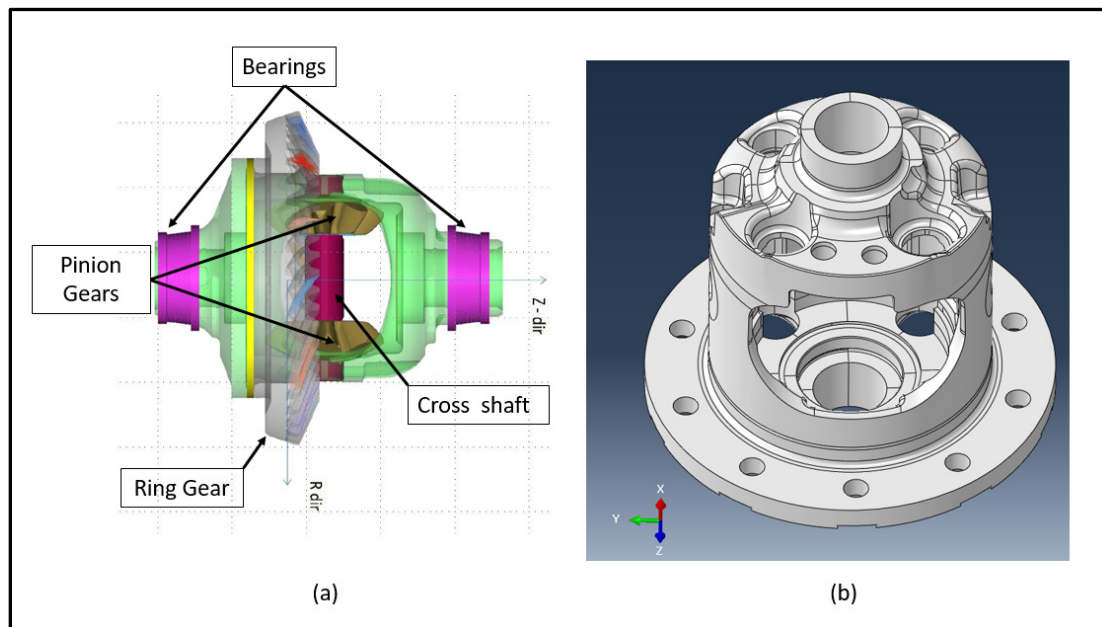


Figure 1: (a) Differential assembly (AAM 2018) (b) Case (Eaton 2016)

A ring gear is bolted to the flange of the case. It is meshed with a pinion gear connected to the engine transmission. The torque from the ring gear is transmitted to the cross shaft through the differential case. The case experiences torsional, bending, gear thrust and axial loads. The case is supported on the axial housing by bearings.

## 1.2 Terminology

Figure 2 shows different regions labeled. The ring gear body is simulated without the tooth profile. This is not significant as the ring gear is bulky and stiff. Dummy bodies are created to simulate the contact at cross-shaft region. Internal gears are not modeled. Instead, their forces are applied on the contact surfaces.

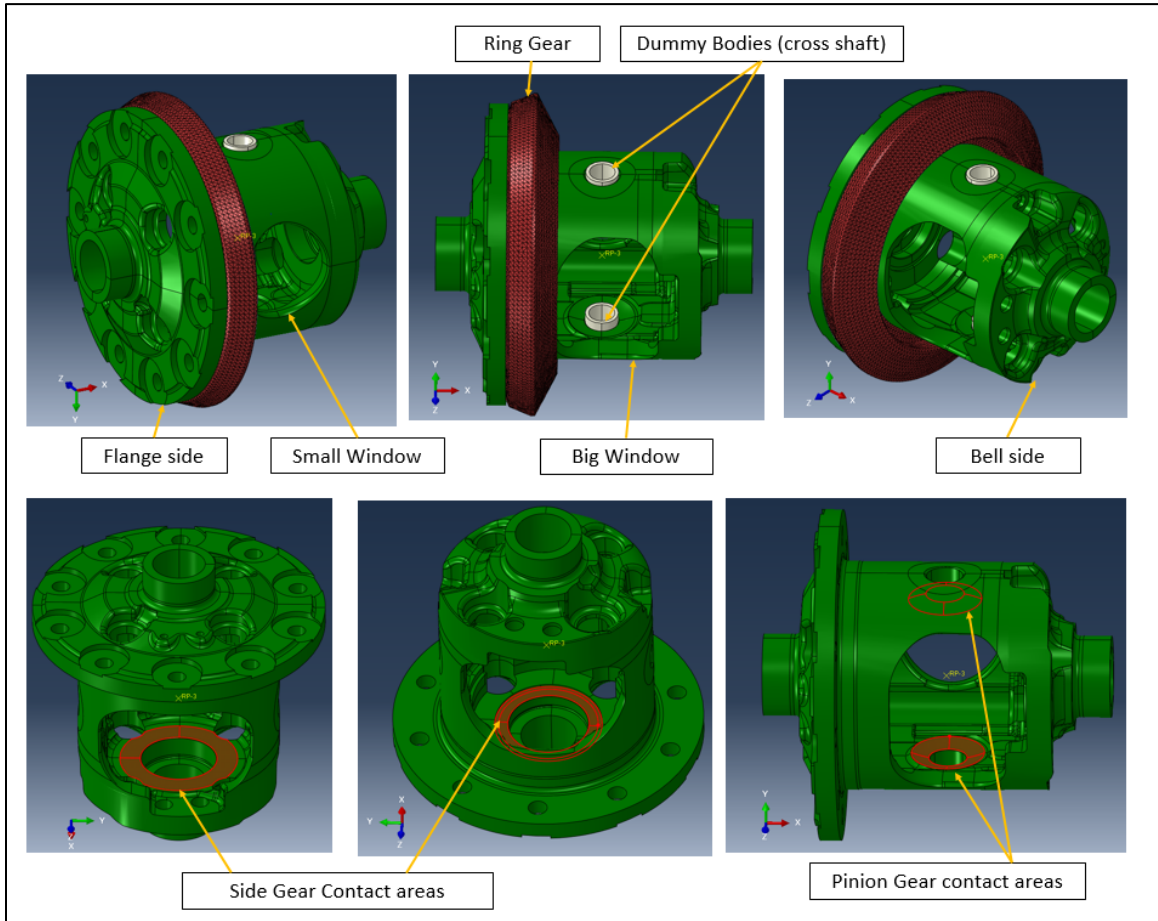


Figure 2: Differential case regions

## 1.3 Objective and scope of work

The main objective of this project is to reduce the weight of the differential case by at least 25% while meeting strength and durability requirements. The process is carried in two different phases, topology optimization and static finite element analyses.

### 1.3.1 Topology Optimization

In the 1<sup>st</sup> phase, topology optimization technique is used with manufacturing constraints to obtain optimal material distribution. A design is generated for maximum stiffness using a

constrained fraction of bulk volume. A total of 72 load cases (36 each in forward and reverse scenarios) were analyzed. Altair Optistruct is used as the solver. The obtained crude geometry is then refined manually to create a feasible design.

### 1.3.2 Static Stress and Fatigue Analyses

In the 2<sup>nd</sup> phase, the refined geometry is parametrized and analyzed for static stress and fatigue life to qualify as per the design criteria. ABAQUS solver is used. The stress history of each surface element is then used to calculate fatigue damage and life.

A multi-axial critical plane approach is adopted [6] to analyze the High Cycle Fatigue (HCF) life. A MATLAB code is developed to search for fatigue fracture plane, critical plane, fatigue damage and life (number of cycles). Python scripts were developed to export stresses from ABAQUS and import fatigue life calculations from MATLAB. This facilitates visualization of all failure locations and not just the most critical one.

## 1.4 Design Criteria

The maximum torque transmitted is 5,875 N-m. The requirement is that there shouldn't be any yielding at 5650 N-m torque (AAM 2018 [8]). The yield strength of the new ductile iron is determined to be 483 MPa. Maximum principal stresses shouldn't exceed this limit. In few local regions, high stresses above 483 MPa cannot be avoided and are observed in the original design. At these locations, the target is set such that stresses in the new design do not exceed those in the original design by more than 10 %. This comes from the assumption that the newer material properties improve by at least 10%. At the time of writing this report, the new yield strength data is not available, hence, 10% improvement in strength is assumed. Although fatigue life requirements are not specified, high cycle fatigue analysis is carried out to identify potential fatigue failure regions.

## 1.5 Material Model

A linear elastic material model shown in

Table 1 is used. Material properties are obtained from Matweb [2].

Table 1: Material properties - DI 7003

<b>DI 7003 – Ductile iron properties</b>	<b>Value</b>
<b>Young's modulus (MPa)</b>	167,000
<b>Poission's ratio</b>	0.275
<b>Yield strength (MPa)</b>	483



## 1.6 Loading and Boundary Conditions

The load path of the differential case is as follows – applied force on the ring gear pitch circle point creates a torque. This is transmitted to the cross-shaft through the differential case flange and body. There is counter torque from the cross-shaft which transmits torque to internal gears which in turn transfer the torque to axle shafts.

The differential operates in two different loading scenarios. One when the vehicle moves in forward direction while the other when the vehicle moves in reverse direction. When the vehicle's in motion, the ring gear contact point (which spans over 2-3 teeth) with the pinion bevel gear, changes continuously. Hence, the ring gear forces are applied at  $10^{\circ}$  intervals. So, the total number of load cases analyzed are 72 (36 each in forward and reverse cases). The effective 'static' load (equal and opposite torques) cause stresses in the differential case.

### 1.6.1 Loading

The differential is analyzed at maximum torque of 5,875 N-m. All units in this report are in metric system N, mm, MPa & Sec. Table 2 and Table 3 show the forces applied on the differential case assembly.

Table 2: Ring gear loads - at 5,875 N-m

<b>Forces</b>	<b>Radial (N)</b>	<b>Tangential (N)</b>	<b>Axial (N)</b>
<b>Forward cases</b>	-33322	-63258	-2545
<b>Reverse cases</b>	9950	63258	-39107

Table 3 : Internal gear and bearing pre-loads

<b>Location</b>	<b>Forces (N)</b>
<b>Pinion gear force - on each Side</b>	15,381
<b>Side gear forces - on each Side</b>	26,150
<b>Bearing pre-load - on each Side</b>	2,224

Figure 3 shows ring gear loads. A cylindrical co-ordinate system is created at the center as shown. The tangential force is applied at pitch circle point (radius 92.75 mm) that causes torque. The spiral profile of the ring gear causes thrust loads in radial and axial directions.

The position of this load on the ring gear changes as the vehicle moves. So, it's applied at  $10^\circ$  intervals. Both forward and reverse cases are analyzed.

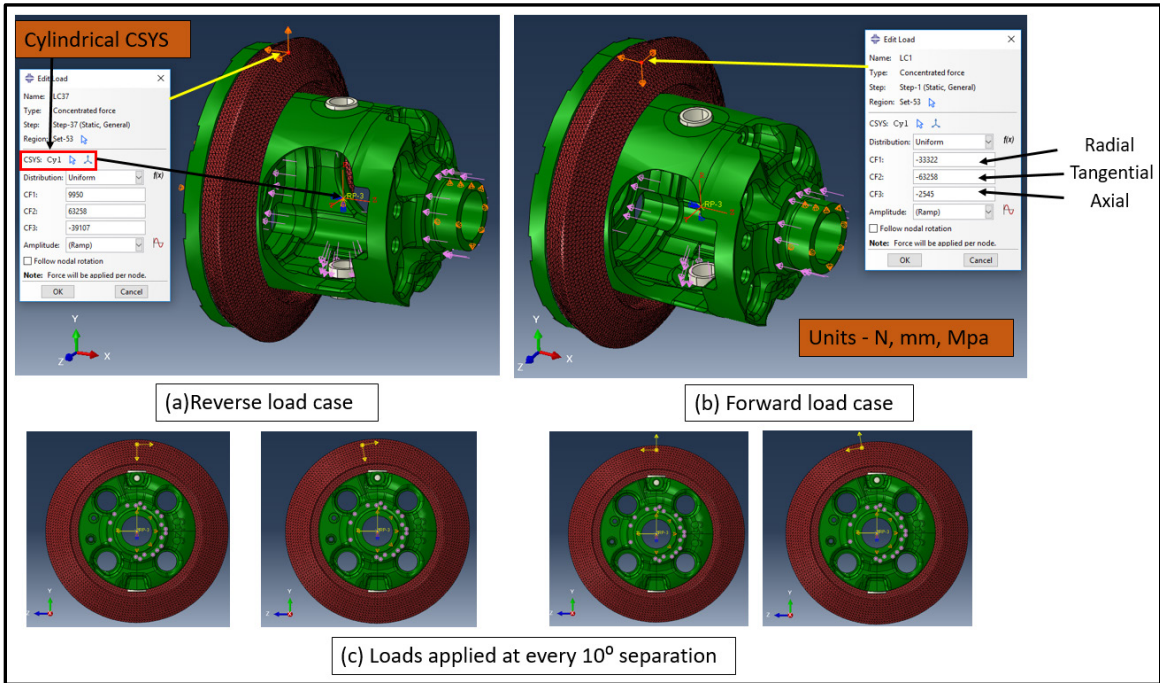


Figure 3: Ring gear loads - a) Reverse cases b) Forward cases c) Loads at  $10^\circ$  interval

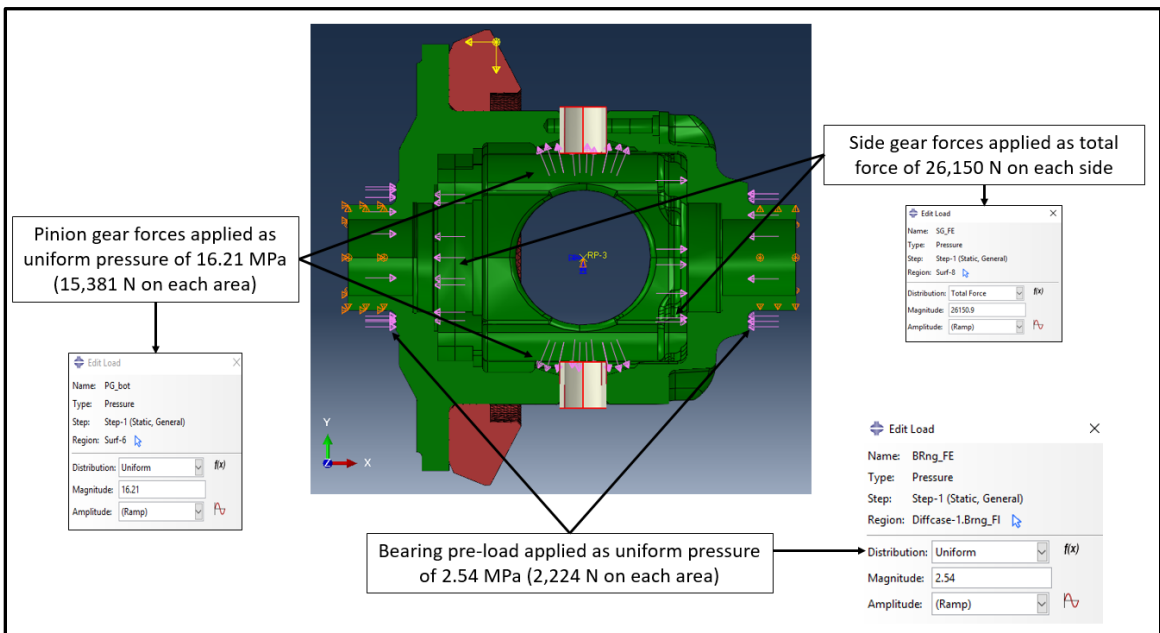


Figure 4 : Internal gear and bearing pre-loads

Figure 4 shows the internal gear thrust loads and bearing preloads. These loads do not change with the position of ring gear load. Hence, they remain constant all throughout the loading cycle in both forward and reverse scenarios.

### 1.6.2 Contacts and Constraints

Figure 5 shows the contacts and constraints defined. Please note that constraints in this context means constraint equations in finite element method and not boundary conditions.

Tie constraint is defined between the differential case flange and ring gear at the bolted interface – These surfaces behave as though they are ‘glued’. A multi-point constraint (MPC) with rigid beam formulation is defined between the center point and internal surfaces of dummy bodies. This can be visualized as the dummy bodies being controlled by a center master node. Boundary conditions are then applied to this master node. A frictionless contact with small sliding formulation is defined between dummy bodies and the differential case. Since large amount of sliding is not anticipated at this interface, small sliding formulation in ABAQUS helps to reduce run time.

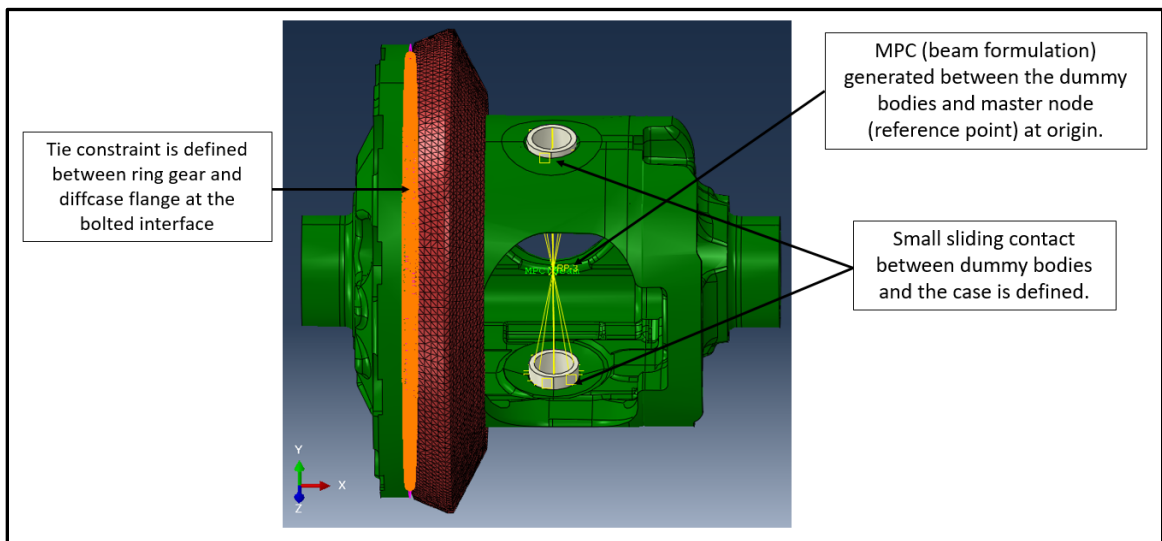


Figure 5 : Contacts and Constraints

### 1.6.3 Boundary Conditions

Figure 6 shows the applied boundary conditions. These conditions are applied with respect to a cylindrical co-ordinate system at the origin as shown. The differential case is supported on the axle housing using bearings shown in Figure 1. Hence, it can rotate at these ends. The flange end bearing surface is fixed in axial and radial direction ( $U_r = U_z = 0$ ). The bell end bearing surface is fixed only in radial direction ( $U_r = 0$ ).

The master node used to control dummy bodies is fixed only in X & Z-rotation and Y-translation ( $U_{rx} = U_{rz} = U_y = 0$ ) with respect to global co-ordinate system (refer to the

triad in Figure 6). The constrained X-rotation opposes the torque. Z-rotation and T-translation constraints are for stability purpose in FEM. They do not see any reaction forces or moments. All unconstrained DOF are free to translate and rotate.

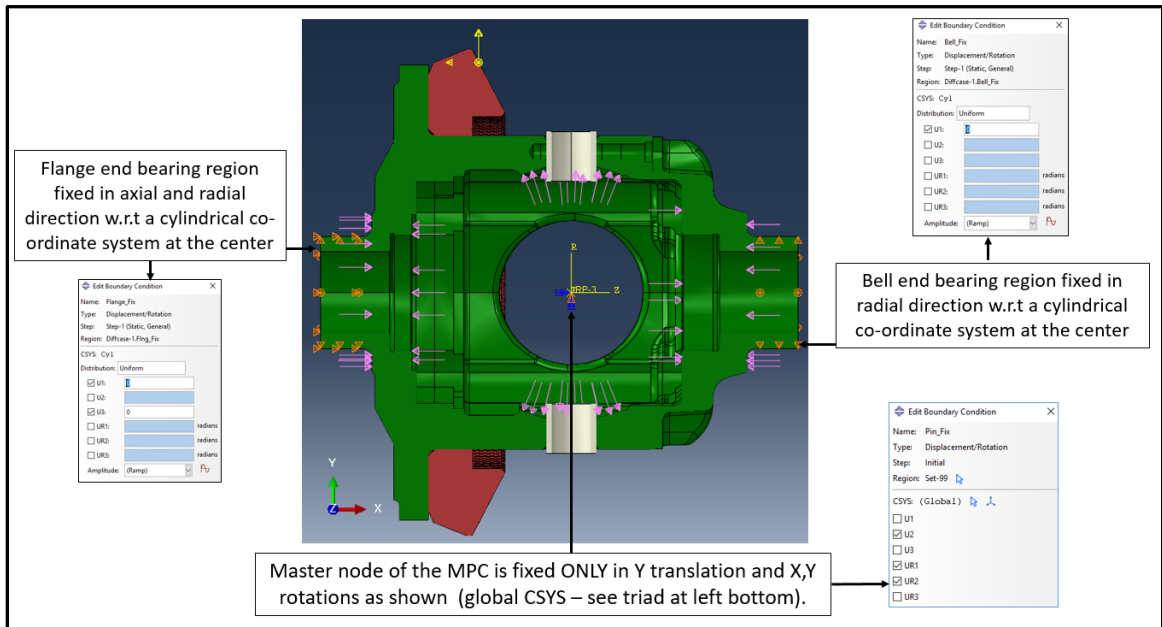


Figure 6 : Boundary conditions

## 2 Initial Analysis

The baseline case is analyzed to identify critical locations, critical load steps and to compare future design iterations with. mesh convergence check is done to ensure that the stresses are converged.

### 2.1 Results

Figure 7 and Figure 8 show the von-Mises stress plots. The contours are capped at 450 MPa. Stresses exceeding this level are shown in grey. Critical regions are labeled as shown. Plots show different failure locations at several load steps.

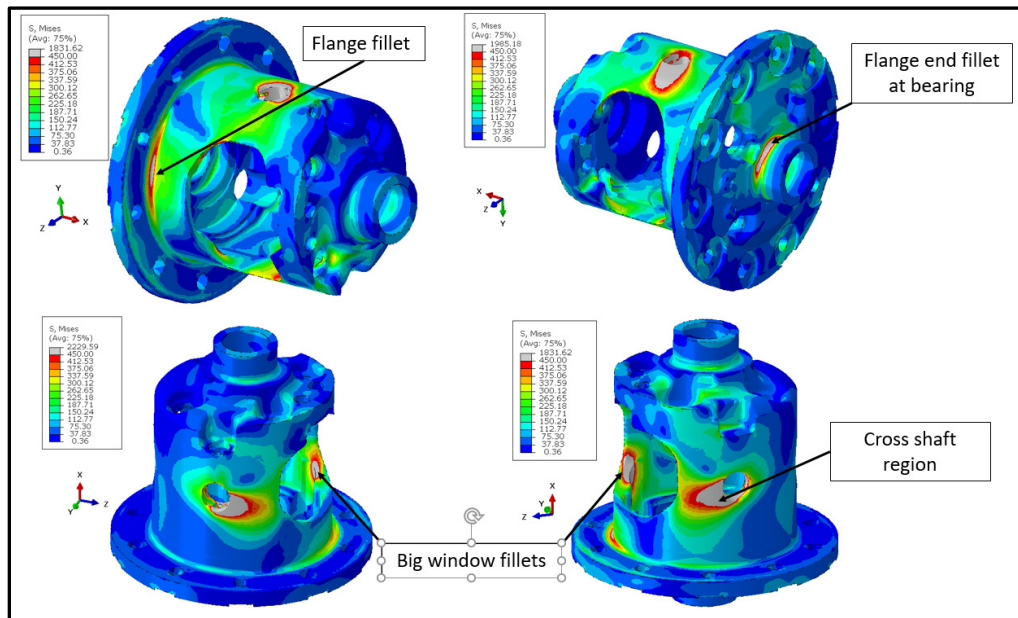


Figure 7 : Critical Locations – 1- von Mises stress plots

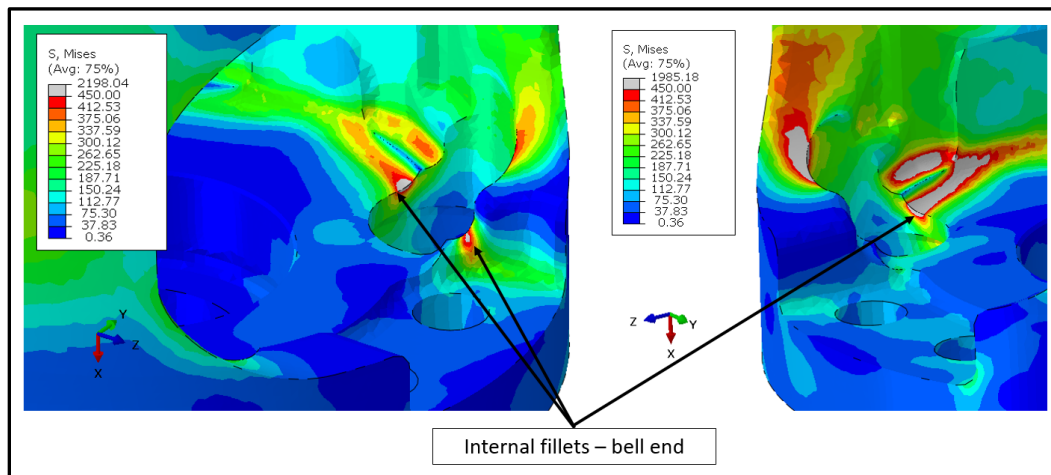


Figure 8 : Critical locations – 2 - von Mises stress plots

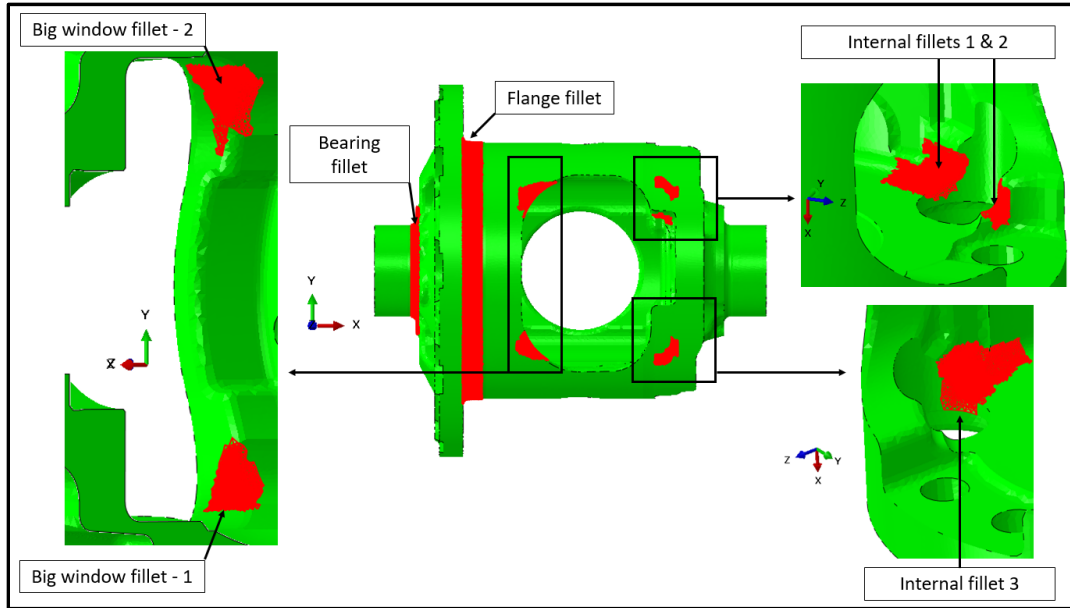


Figure 9 : Element sets at critical locations

Figure 9 shows the element sets created in red. This is done to identify the maximum von-Mises stress history at these critical locations. Python scripting in ABAQUS is used to extract maximum stress at each location which is plotted in Figure 10. Note that there are several elements in each set. The maximum stress element in each set is not constant for each step. Hence, the obtained curves are not smooth in all cases. The 450 MPa line helps identify critical load steps.

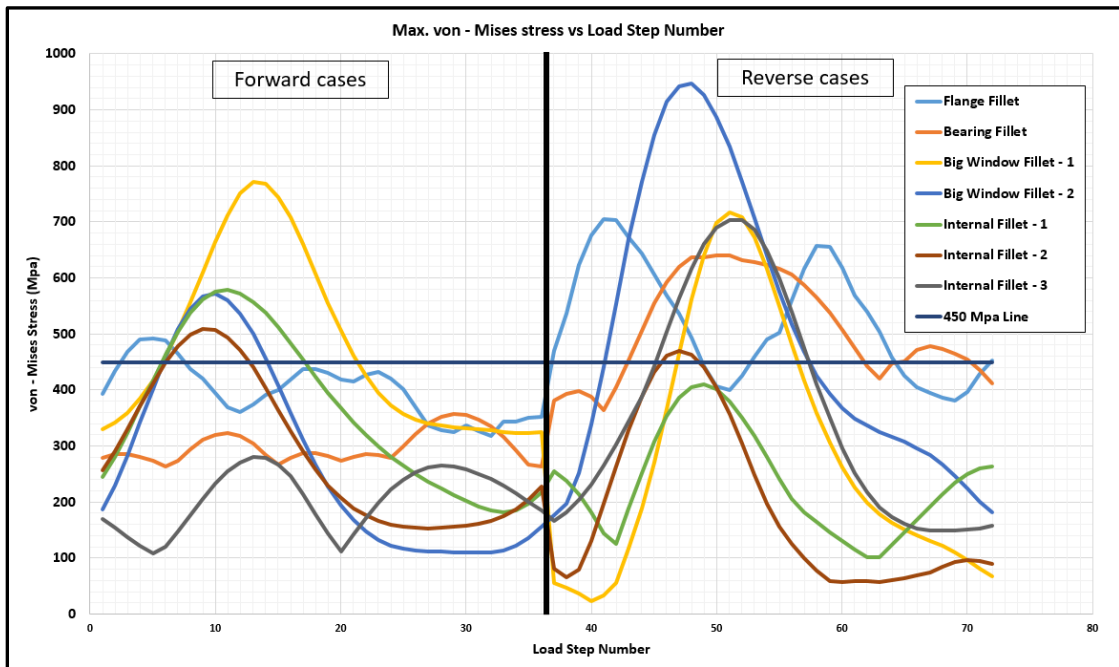


Figure 10 : Max. von-Mises stress at all critical locations vs step number

## 2.2 Mesh Quality

Table 4 shows the element quality criterion. Stringent values are used compared to general suggested criterion [3]. Any element that violates these criteria should be warning elements (shouldn't be in significant number) and not error elements. Figure 11 shows the highlighted elements (in yellow) that do meet the criterion in Table 4. These elements are not present in large numbers or at any critical locations. Table 5 describes mesh statistics in which it is shown that the percentage of these elements is very low. No error elements were present.

Table 4 : Element quality criteria

Metric	Value
Shape factor	<0.1
Tri-face corner angle	<5 & > 170
Aspect ratio	>5
Shortest edge	<0.01 mm

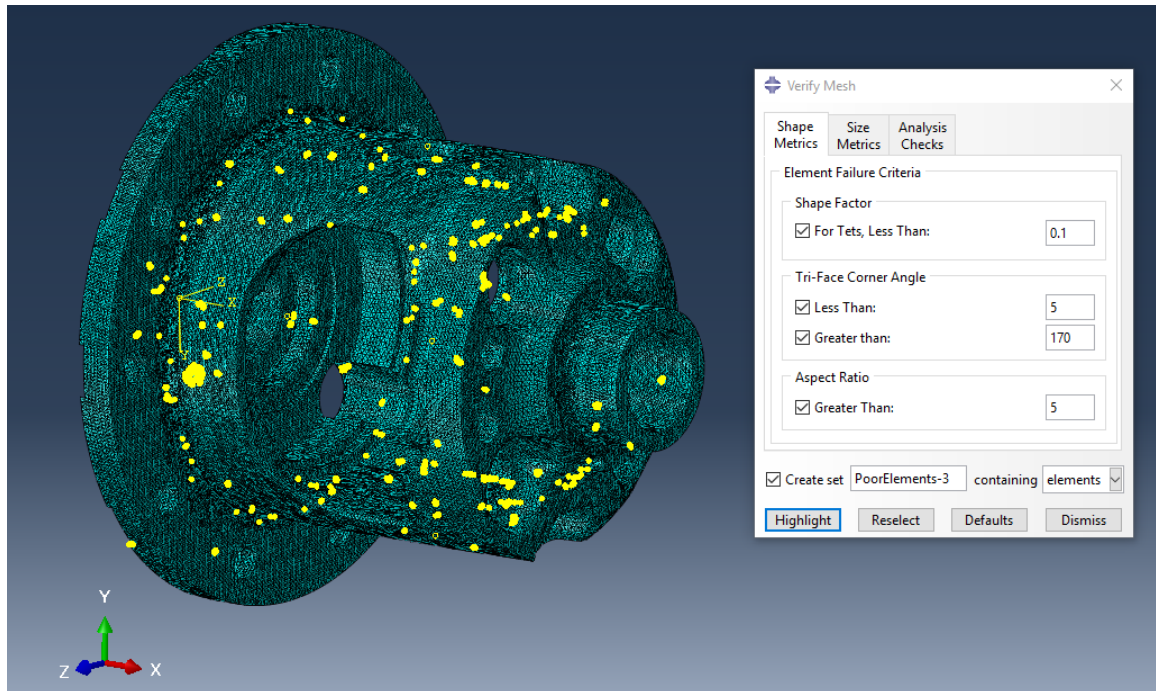


Figure 11 : Mesh plot showing warning elements (yellow)

## 2.3 Mesh Convergence

In the previous section critical locations and load steps at which maximum von-Mises stresses are observed. Using this data, mesh convergence is done at these locations at their respective critical load steps.

Mesh sizes ranging from 0.75 mm to 0.125 mm are locally applied at these locations and model is meshed. Figure 11 shows the zoomed mesh plots with different local mesh sizes.

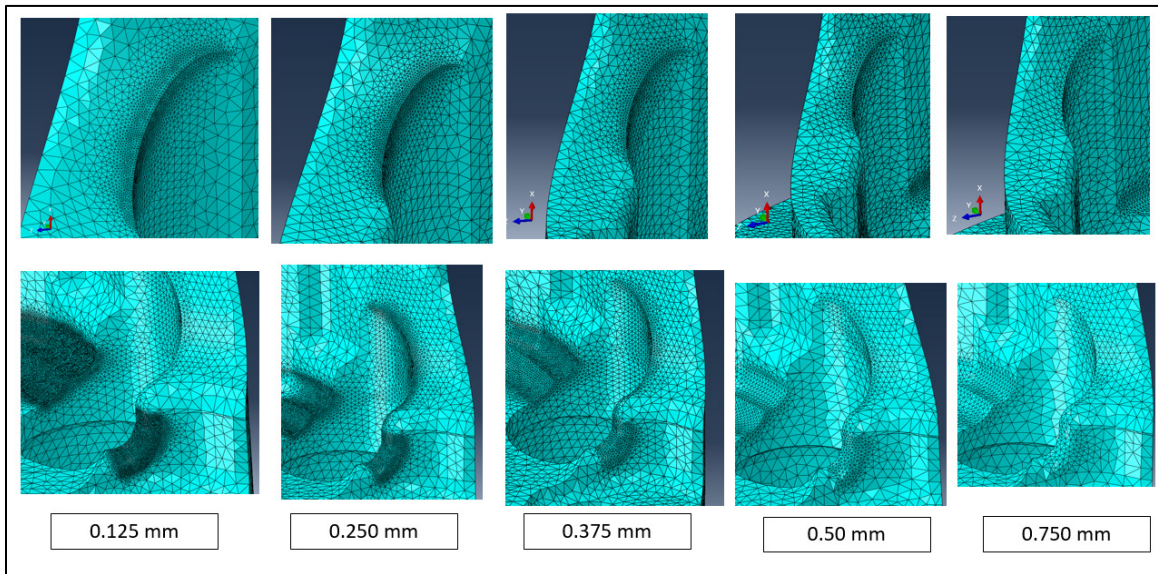


Figure 12: Zoomed mesh plots

Table 5: Mesh statistics

	Local mesh Size (mm)	Global mesh Size (mm)	No. of nodes	No. of elements	% Warning elements
<b>Model -1</b>	0.75	1.85	279,561	1,462,492	0.014
<b>Model -2</b>	0.5	1.85	377,042	1,978,812	0.011
<b>Model -3</b>	0.375	1.6	483,570	2,563,267	0.008
<b>Model -4</b>	0.25	1.6	617,117	3,262,318	0.006
<b>Model -5</b>	0.125	1.5	1,119,410	5,846,390	0.007



### 2.3.1 Mesh convergence study results

Figures 13 – 18 show the max. von – Mises stress at each critical location vs mesh size and percentage difference vs mesh size. Convergence is checked at multiple locations at multiple load steps. The convergence criteria are assumed to be satisfied when the percentage difference between von-Mises stress reaches below 5% compared to the previous mesh size. Although the percentage differences show jagged trends, local mesh size of 0.5 mm, in most cases provides reasonably good results. This is chosen as the run times with mesh sizes .375 and 0.25 mm are high (more than 48 hours for all 72 load steps).

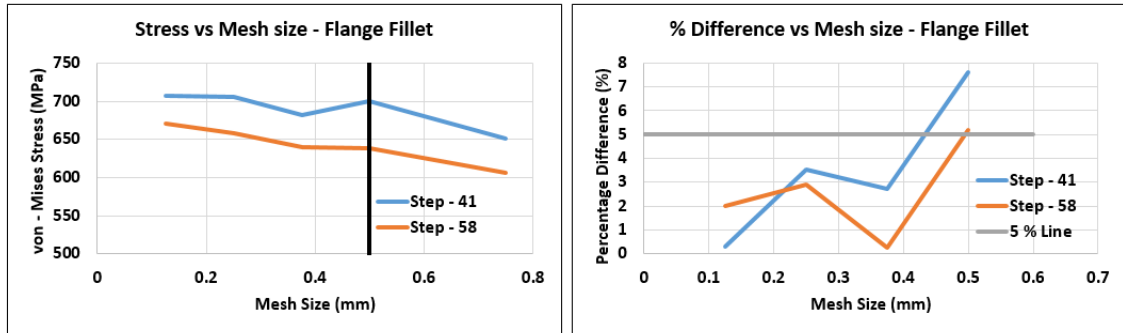


Figure 13 : Stress and percent difference v. mesh size - Flange Fillet

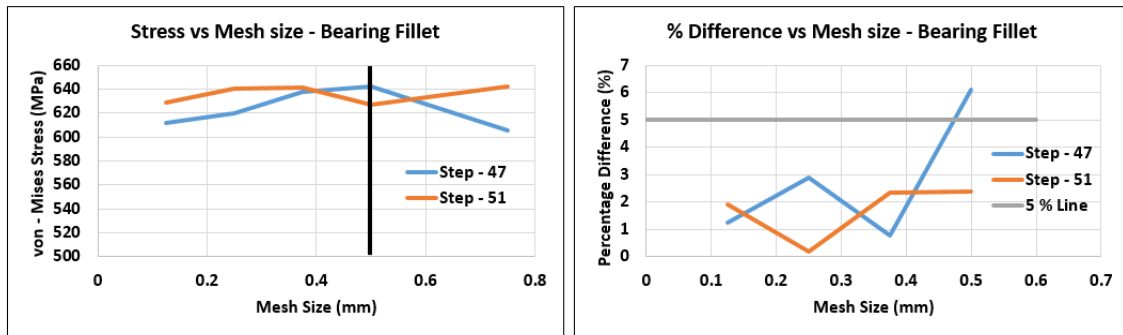


Figure 14 : Stress and percent difference v. mesh size - Bearing Fillet

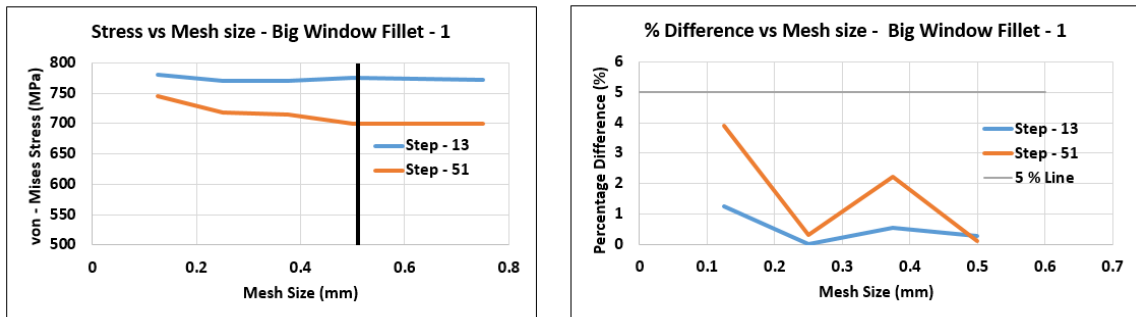


Figure 15 : Stress and percent difference v. mesh size - Big window fillet - 1

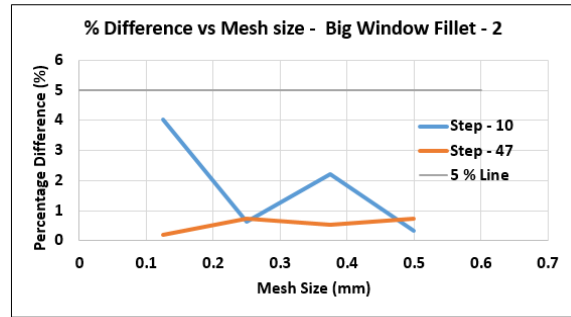
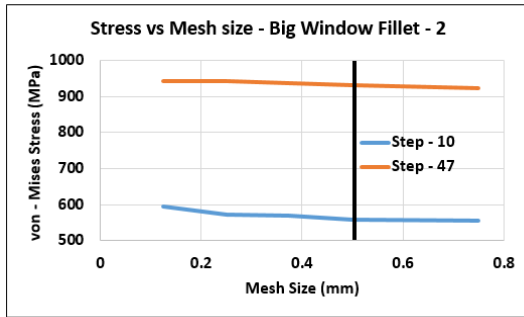


Figure 16 : Stress and percent difference v. mesh size - Big window fillet - 2

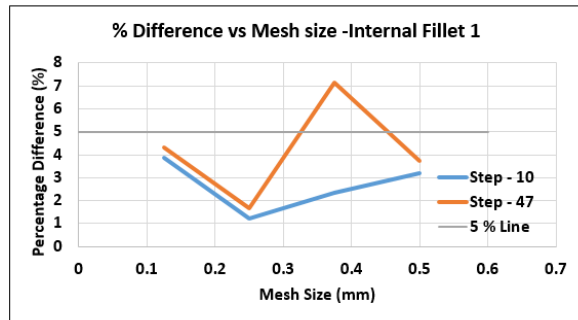
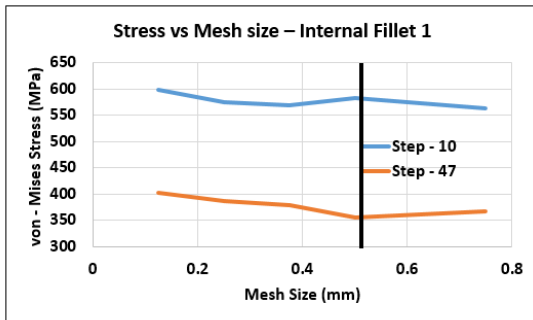


Figure 17 : Stress and percent difference v. mesh size - Internal fillet - 1

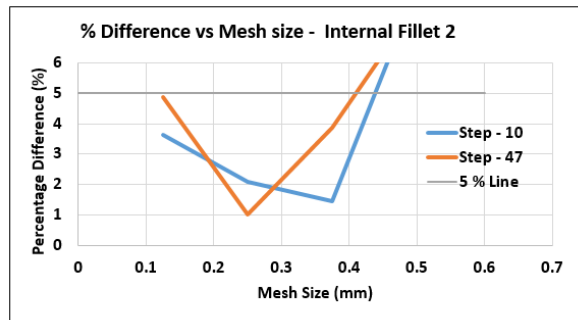
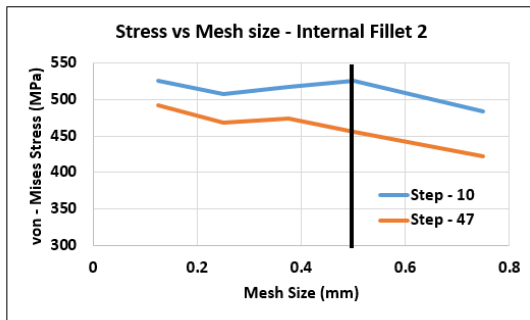


Figure 18 : Stress and percent difference v. mesh size - Internal fillet - 2

## 3 Topology optimization

Topology optimization is one of several optimization techniques used to find optimal material distribution. With advancement in computational power and cutting-edge algorithms, optimization can be done within a reasonable time.

### 3.1 Theory

A basic optimization problem is finding minima or maxima for a given curve subjected to a set of constraints.

For example [4],

Minimize  $f(x) = f(x_1, x_2, \dots, x_n)$  – objective function

Subjected to  $g_i(x) \leq 0 \quad i = 1, 2, \dots, m$  – constraints

$$a \leq x_k \leq b$$

Here,  $f(x)$  is the objective function,  $g_i(x)$  is a set of constraints and  $x_k$  are the design variables. The function is numerically optimized by the software using gradient based or heuristic approaches.

In the scope of structural optimization, an example problem can be defined with the objective of minimizing mass of an object while constraining deflection, stress, or natural frequency.

#### 3.1.1 Definitions

Any optimization problem requires the following.

- Design variable
- Responses
- Constraints
- Objective

A **Design variable** can be defined as a parameter that can be varied to optimize the model

**Responses** are functions that need to be evaluated. These include an objective function and multiple functions upon which constraints can be placed

**Constraints** are equations that all response functions except the objective function/response are subjected to.

An **Objective** function is the main function that needs to be minimized or maximized.

### 3.1.2 Structural Optimization

Topology optimization problems are solved using density or SIMP method (Solid Isotropic Material with Penalization) methods [4] & [5] by the optimizer. Element density ( $\rho$ ) here refers to a parameter that each element in the FEM model is assigned. The value of  $\rho$  varies from 0 to 1. This parameter is used to penalize the stiffness of the element using the following power law equation.

$$K(r) = \rho^P K \quad \text{-(from [4])}$$

Where  $K(r)$  is the penalized and  $K$  is the original stiffness matrix.  $P$  is a penalizing factor which is greater than 1 (usually between 2 and 4) [4].

The density of each element is a design variable. Responses are evaluated after penalizing stiffness of each element for various values of  $\rho$ . Through iteration, this determines the ‘importance’ of that element. Finally, densities where the given objective function that is subjected to given constraints is satisfied are determined. Ideally, the stiffness of element should be 0 or 1 times the original element stiffness, indicating presence or absence of the element. But, numerically it is not possible to solve with such factors. Hence, power law method is used. Intermediate density values mean softer material is placed. Although this doesn’t reflect reality, a good material distribution can be obtained.

## 3.2 Optimization method

Altair Optistruct is chosen as the solver. Initial analysis in section 2.1 helped identify critical regions. This information is used in the optimization process as well. The main aim is to reduce the mass of the differential case. The optimizer is instructed to minimize strain energy of critical regions while constraining the total volume of the model. The optimization functions are defined as follows.

### 3.2.1 Design variables

Features on flange and bell ends that were not critical to the functionality are removed and filled with bulk material as shown in Figure 19. The bulk material is then defined as the design volume/space (in cyan and pink) containing design variables. The elements in non-Design space are not penalized. The densities of these elements in design space are varied in iterations by the optimizer to determine optimal material distribution.

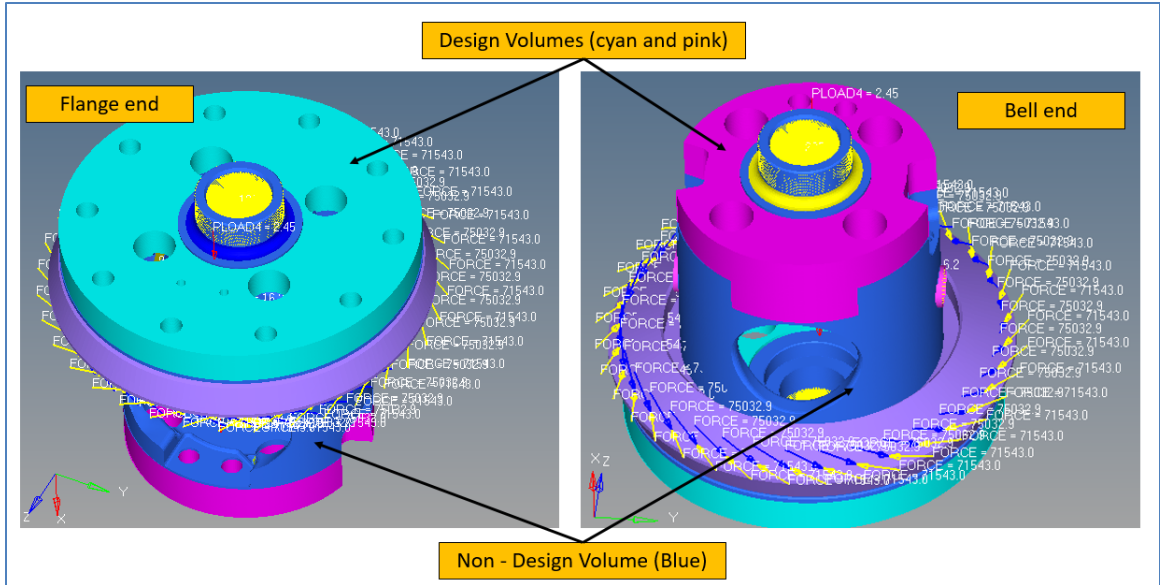


Figure 19 : The volumes at flange and bell ends constitute the design space

### 3.2.2 Responses

The optimizer evaluates the defined responses in every iteration to monitor and predict variables.

Volume fraction is defined as one of the responses. When the density of each element is varied between 0 and 1, in each iteration, the effective volume is calculated by multiplying actual volume of the element by the density. Volume fraction is the ratio of effective volume in an iteration and the initial total volume.

Weighted local compliance of regions shown in Figure 20 is defined as another response. Compliance is defined as flexibility or inverse of stiffness. Collectively, the total compliance of the local regions is calculated by the optimizer using strain energy. If strain energy is more in the local regions, then compliance is high and vice versa. In this case, there are 72 load steps, hence total weighted total compliance is to be used. It is defined by the following equation.

$$C = (w_1 * C_1 + \dots + w_{72} * C_{72}) / (w_1 + \dots + w_{72})$$

Where  $C$  is the total weighted compliance,  $C_n$  is the total local compliance at  $n$ th load step and  $w_n$  is the weight assigned to that load step. In this analysis, all weights are given the value 1.

In Optistruct, local compliance can be defined for each load step using DRESP 2/L and weighted compliance using DEQUATION 'cards' as shown in Figure 21.

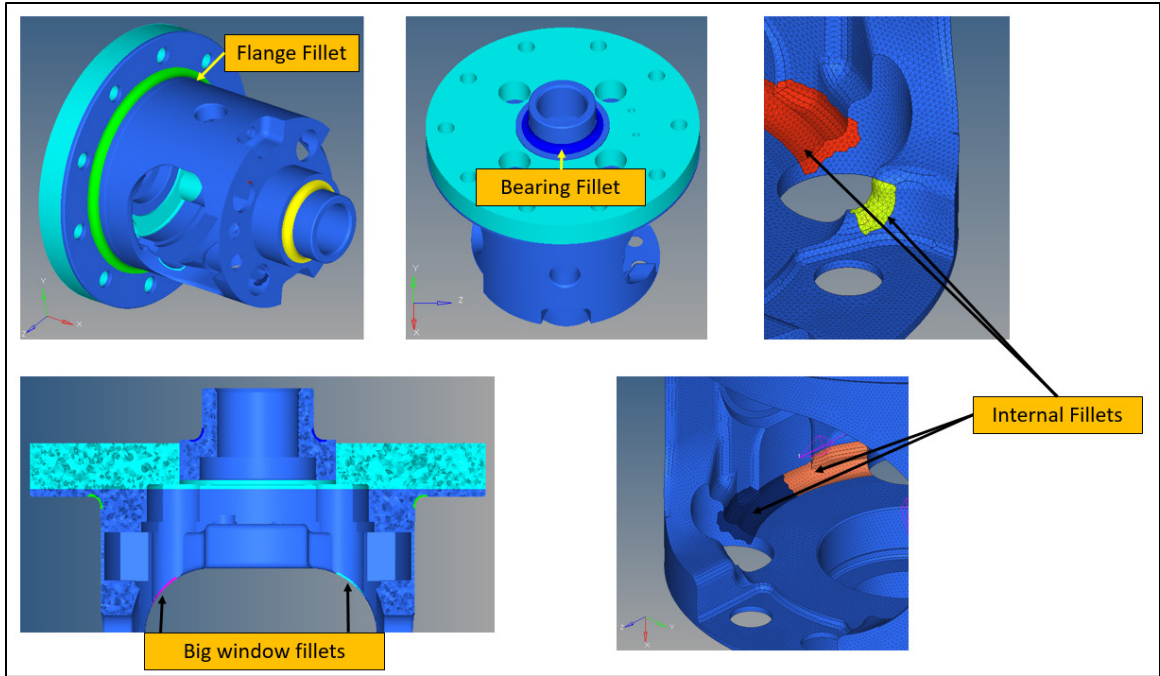


Figure 20 : Critical regions for which local compliance response is defined

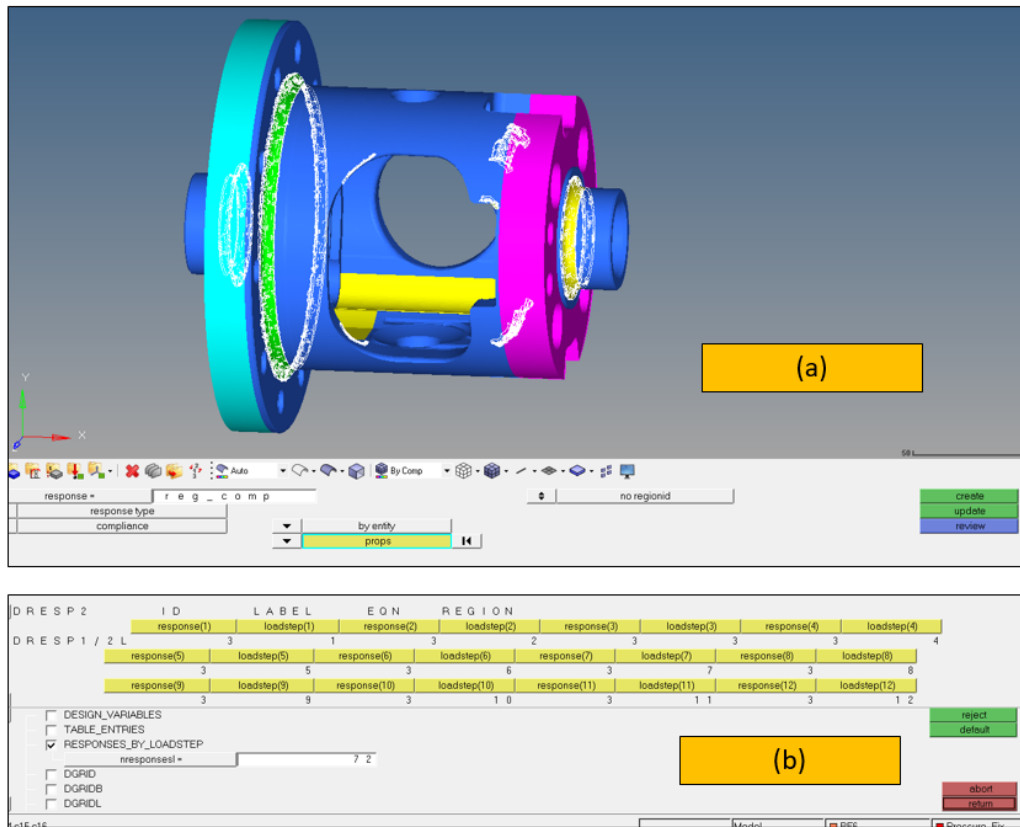


Figure 21: FEM settings - a) Compliance response regions (in white); b) DRESP 2/L card

### 3.2.3 Optimization Constraints

A constraint is placed on the volume fraction. The condition is that the final volume fraction should not exceed 35% of the bulk, initial volume.

A manufacturing constraint to produce a design that will allow the casting die to be pulled is defined by setting a draw direction.

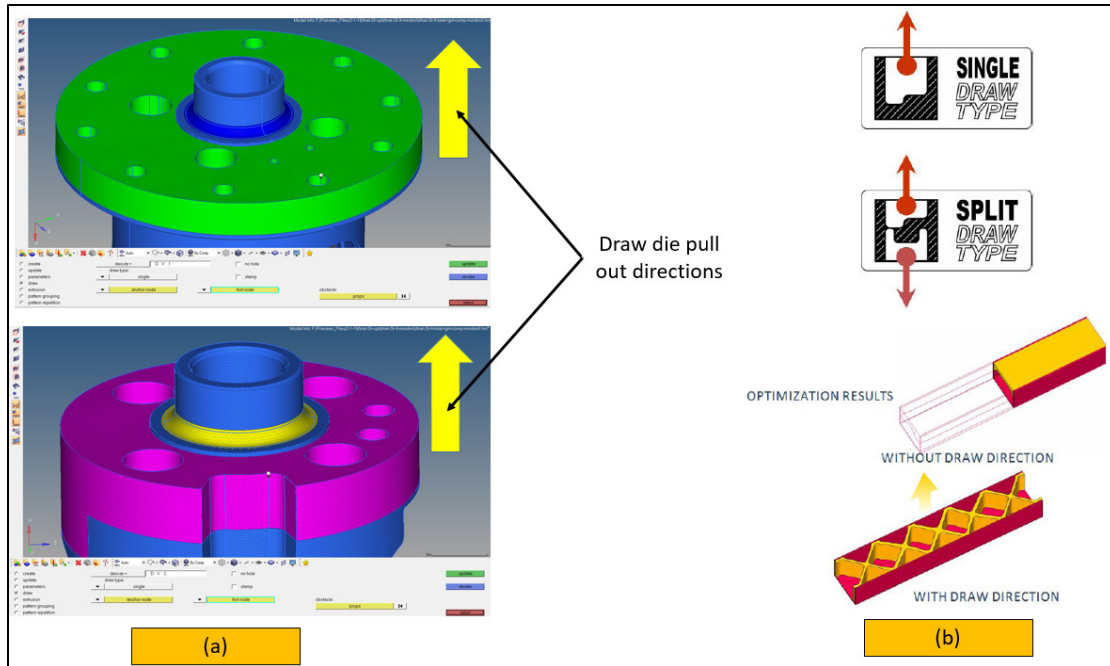


Figure 22: a) Die pull out direction constraints b) Example of draw constraints from [4]

Also, a minimum member size of 5 mm is defined using MINDIM ‘card’ in optistruct.

### 3.2.4 Objective Function

The Objective is set to minimize weighted local compliance of regions (elements) shown in Figure 20. Minimizing compliance is synonymous with minimizing strain energy. So, the objective is to generate a design that minimized strain energy in critical areas while using only 35% of the initial volume.

## 3.3 Optimization Results

The optimizer solves all load cases in each iteration and finally outputs element densities that satisfies the objective. Element densities can be plotted in Hyperview that show the optimal material distribution. Figure 23 shows element density plots capped at 0.45 value. This value is not particularly of significance and used to visualize.

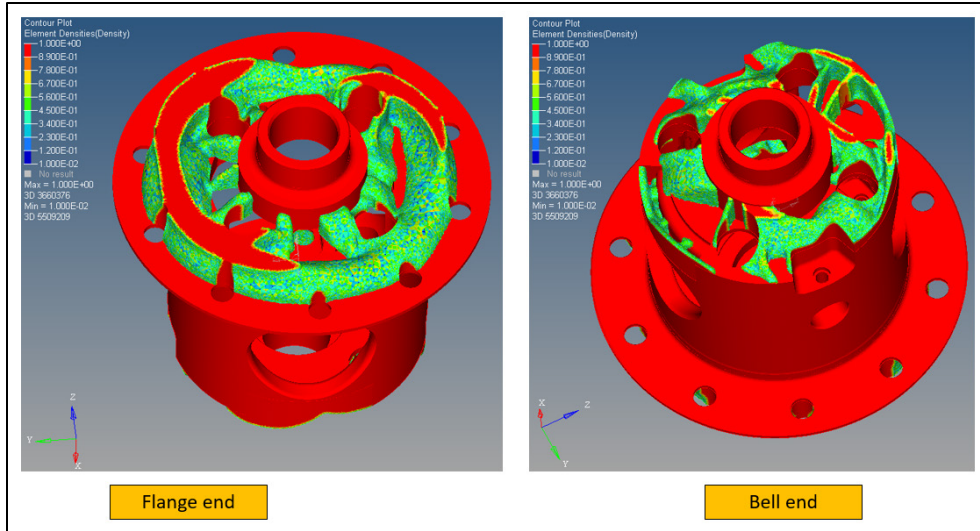


Figure 23 : Topology results - element density plots

### 3.3.1 Geometry refinement

The obtained topology from Optistruct is crude and often impractical to manufacture due to irregular topology. Hence, it is exported to a CAD software. In this project NX 11.0 is chosen as CAD tool. The imported topology is refined to create manufacturable geometry. The new geometry is parametrized to finalize dimensions. Due to complex topology, the created geometry does not exactly match the obtained topology. A few approximations were made to create feasible geometry.

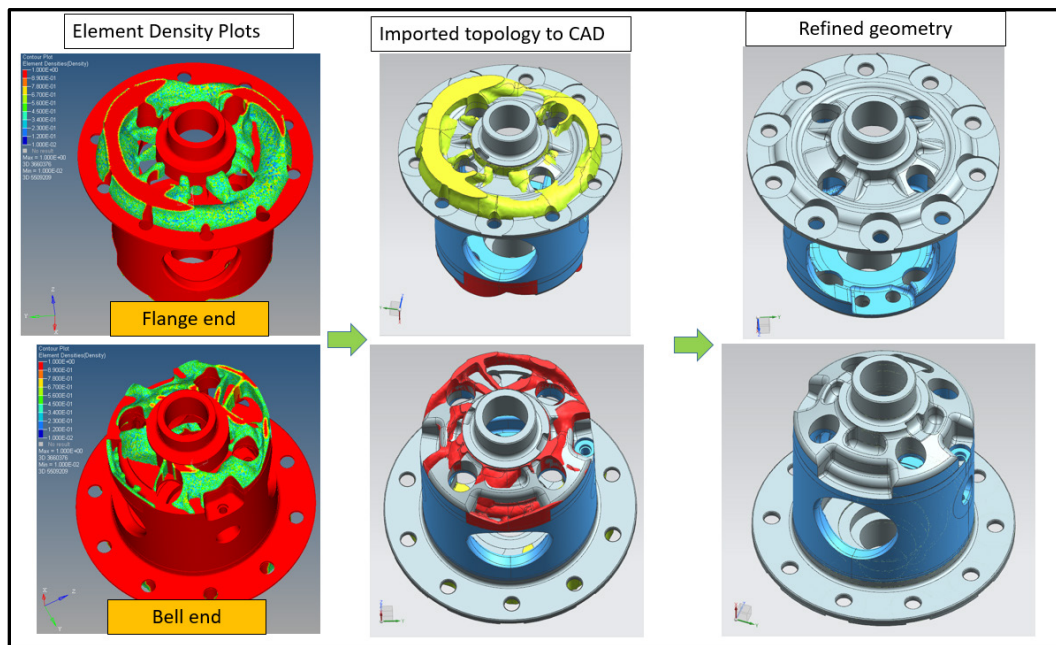


Figure 24 : Geometry refinement process



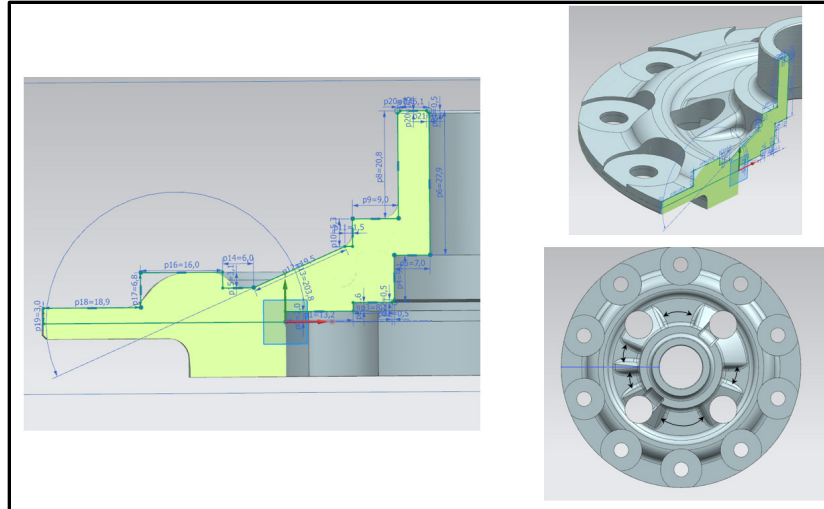


Figure 25 : Parametrized geometry - flange end

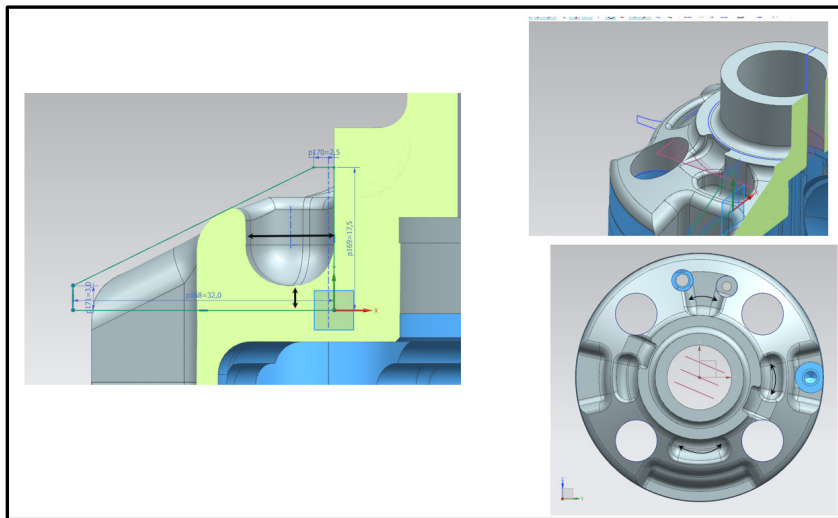


Figure 26 : Parametrized geometry - bell end

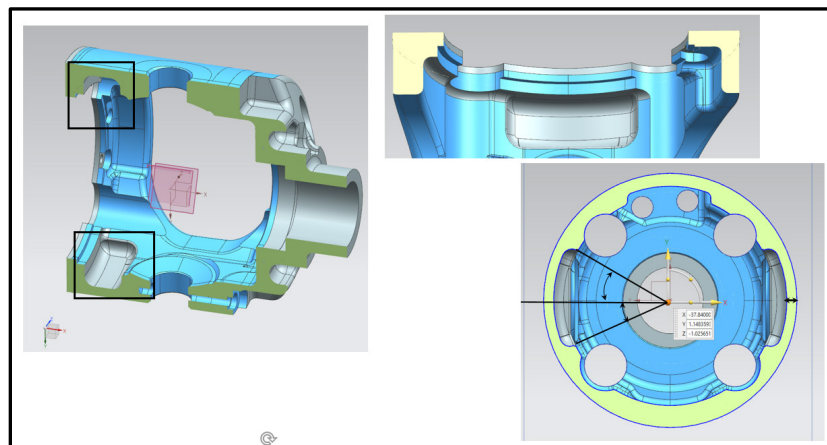


Figure 27: Parametrized geometry - barrel region

Figures 25-27 show different regions where dimensions are parametrized. Note that during topology optimization, only flange and bell end regions were optimized. Due to difficulty in including manufacturing constraints at barrel region, it is not optimized in topology optimization. However, during manual tweaking, some material in the barrel region was removed as shown in Figure 27. This will not affect the optimized topology at bell and flange ends as it is far away from those design volumes.

## 4 Re-Analysis

### 4.1 Results

In the previous section, the obtained topology only satisfies maximum stiffness/minimum compliance criterion. It must be further tweaked to ensure stresses at critical locations are not exceeding the limit. It is done manually in few iterations by analyzing again in ABAQUS.

Because of the high number of parameters, the sensitivity study of each parameter wasn't feasible. Key parameters were identified, and the dimensions are varied for optimizing. Since material is removed compared to the original design, stresses are bound to increase. In the next few Figures (28-35), max. stress plots are shown at all critical locations with contours capped at 425 MPa. Stresses above this limit are shown in grey region.

It should be noted that the forces listed in Table 2 and Table 3 are at a torque of 5875 N-m, but the design criteria provided by AAM dictates that the stresses are to be evaluated at 5650 N-m torque. Since, these torques are almost same (factor of 0.96), stresses are evaluated at 5875 N-m which result in a conservative analysis. However, if it is needed to strictly adhere to the design criteria, using linear assumption (stress proportional to torque), stresses or safety factor can be scaled by the ratio of torques.

The flange end tweaking was simple as critical regions are not affected by the parameters at this end. The bell end thickness however, affects the stresses at internal fillets (shown in Figure 28). The sub-pictures to the right show stress plot of few elements selected near the critical region to show the maximum local stress over several iterations.

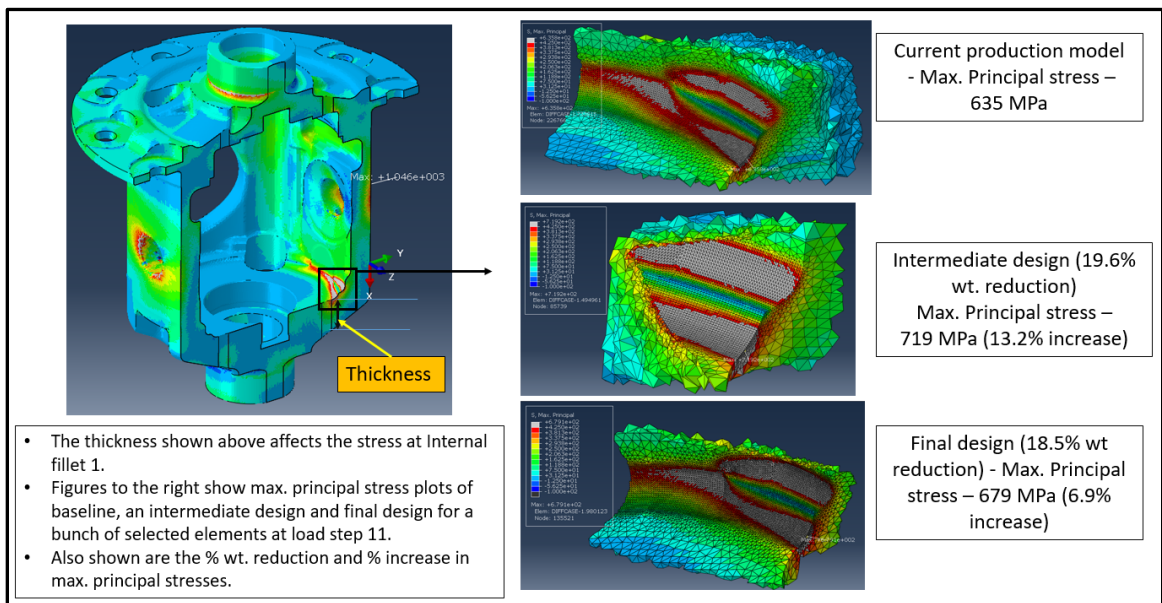


Figure 28 : Max. Principal stress plots - internal fillet 1

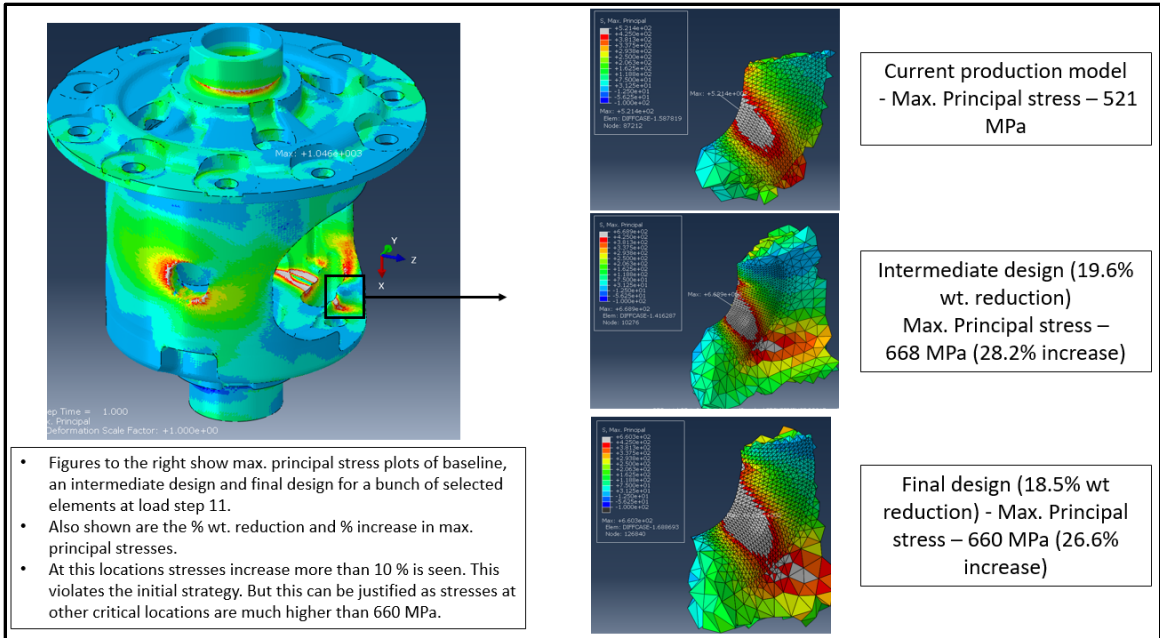


Figure 29: Max. Principal stress plots - internal fillet 2

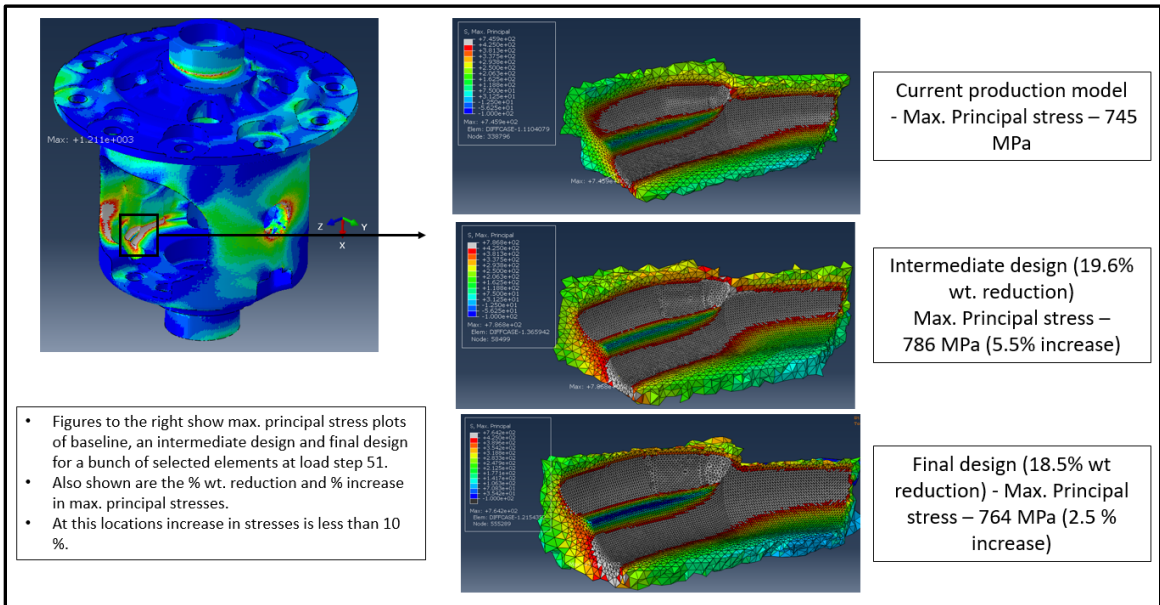


Figure 30: Max. Principal stress plots - internal fillet 3

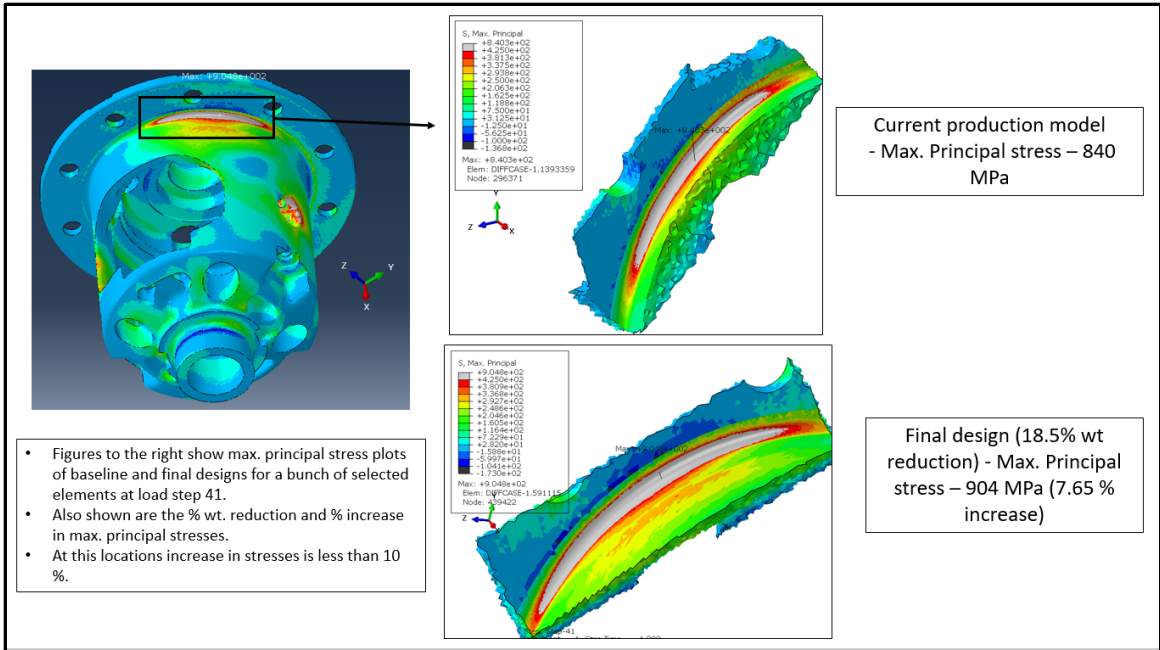


Figure 31: Max. Principal stress plots - Flange fillet

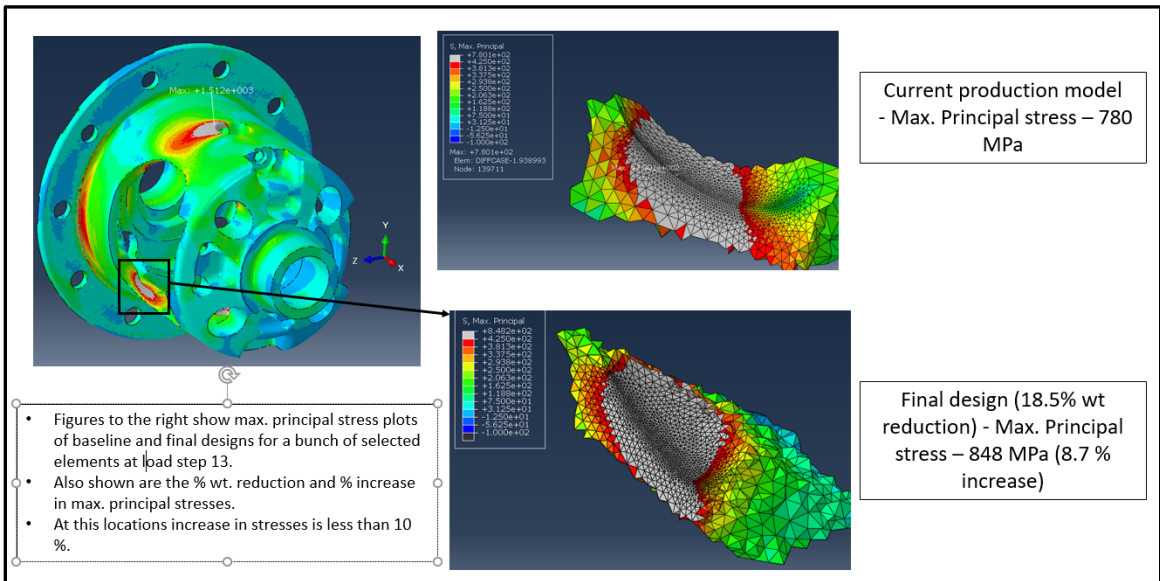


Figure 32: Max. Principal stress plots - Big window fillet 1

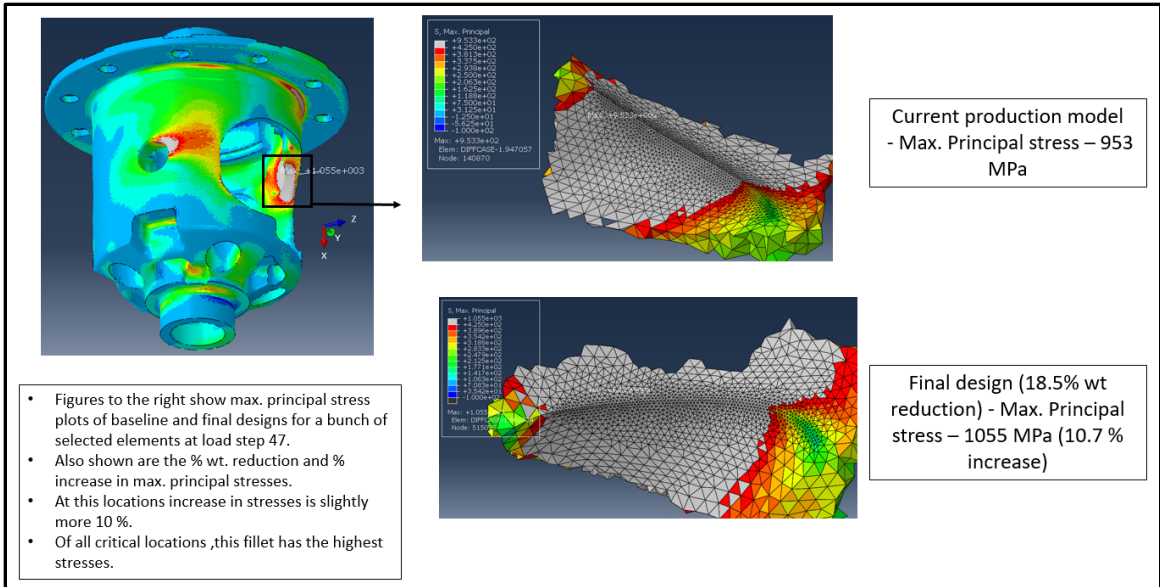


Figure 33 : Max. Principal stress plots - Big window fillet 2

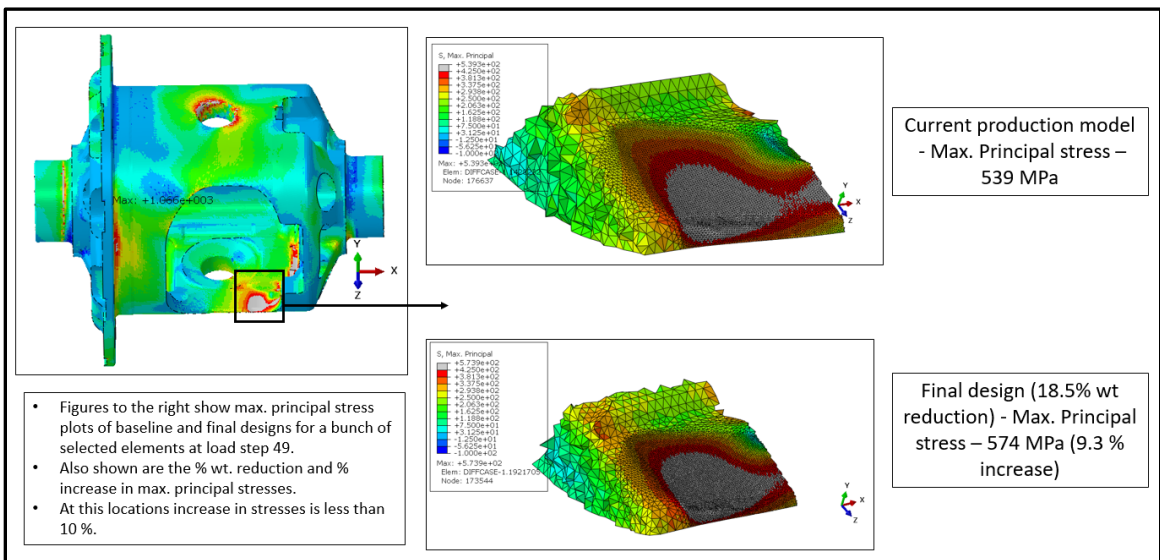


Figure 34: Max. Principal stress plots - Window region

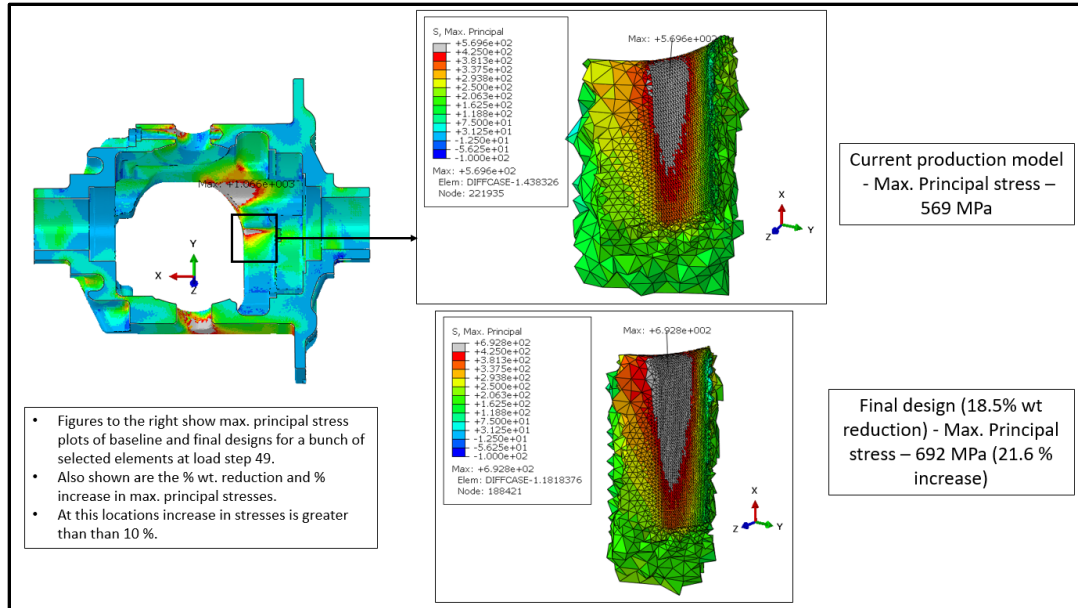


Figure 35: Max. Principal stress plots -Internal corner region

## 4.2 Summary

Table 6 summarizes the max. principal stresses at all critical locations and load steps. Only two locations (Figure 29 and Figure 35) where stresses exceeding 10% compared to baseline are found. These can be justified because max. stresses at other locations are much higher than stresses at these locations. 18.5 weight reduction is obtained. The most critical location is big window fillet 2 at load step 47. Also, upon re-design, it is to be ensured that the center of gravity (COG) shouldn't offset radially in significant amount compared to the original design. In the original design, the COG is radially offset by 2.03 mm while in the new design, it is radially offset by 2.33 mm. The change in COG radial offset is negligible.

Table 6 : Results Summary

Load step	Location	Max. Principal stress (MPa)		% increase in Max. Principal stress
		Current production model	Final design	
11	Internal fillet 1	635	679	6.9
11	Internal fillet 2	521	660	26.6
51	Internal fillet 3	745	764	2.5
41	Flange fillet	840	904	7.64
13	Big window fillet 1	780	848	8.7
47	Big window fillet 2	953	1055	10.7
49	Window region	539	574	9.3
49	Internal corner	569	692	21.6

## 5 Fatigue analysis

Since the differential is a rotating component that experiences cyclic loading, and hence, fatigue analysis is of interest. Fatigue failure is a surface phenomenon and crack initiation occur on the surface. Hence stress histories of points on the surface are enough to compute fatigue life. Although fatigue life requirements are not specified, a high cycle fatigue life analysis is performed.

### 5.1 Surface Stress extraction

It is important to note that surface stresses are 2D in nature in most cases. For 3D elements, accurate stresses can be obtained only at integration points which are not on the surface of the element. To obtain surface stresses, a layer of ‘membrane – M3D3’ elements are created over the existing ‘solid’ elements. Negligible thickness of  $1\mu\text{m}$  is given along with same elastic modulus and Poisson’s ratio as the case. Membrane elements have only 2 in-plane translational DOF and stress output is also of 2D in nature. Their integration points lie on the surface and accurate surface stresses can be obtained. The additional thickness of  $1\mu\text{m}$  has negligible effect on the overall stresses as they impart almost no stiffness. Also, at low thickness values, membrane element stresses are independent of their thickness values. Figure 36 shows the ‘skin’ layered on the surface.

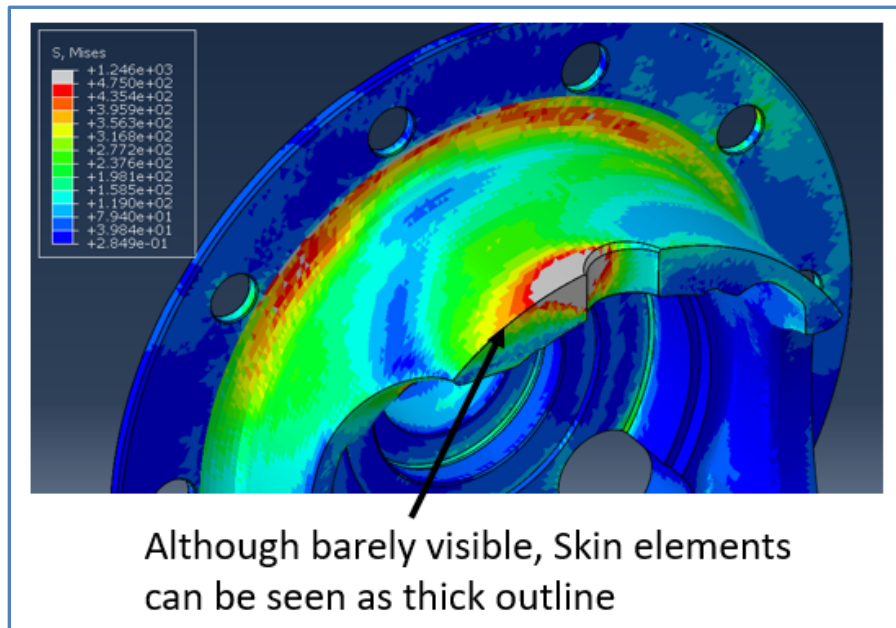


Figure 36 : Membrane elements on the surface

#### 5.1.1 Need for Critical Plane Fatigue analysis

Before getting to the critical plane fatigue theory, it is important to understand uni-axial fatigue. Consider a small element subjected to uni-axial tension-compression cycle as



shown in Figure 37. The stress amplitude can be simply calculated and compared to amplitude in SN curve (eg. Figure 40), to find life.

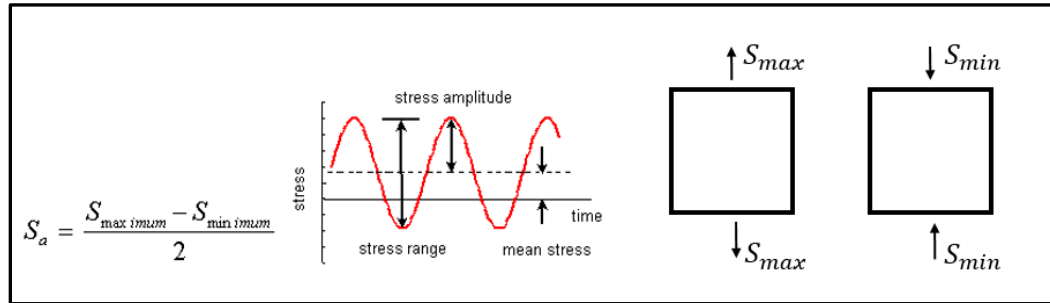


Figure 37: Uni-axial alternating stress example

This is a simple scenario and rarely occurs with real-life loading conditions. Consider an element subjected to three different scenarios each with two load steps. This results in three different stress states as shown in Figure 38. Scenario 1 is the same as explained above. Scenario 2 is slightly complicated in which the element is subjected to bi-axial stresses, but principal axes orientation remains constant during both load step 1 and 2. In such a case, we know that maximum shear stress occurs on a plane inclined  $45^\circ$  to the principal axes and hence, maximum shear stress range occurs on the same plane. So, shear stress range can be calculated easily and mapped on to a SN curve to obtain life. Scenario 3 is like scenario 2 but in this case, principal axes orientation changes. Now the problem is how to calculate a “range” of stress which can be mapped onto uni-axial SN test data. In such problems, the plane with maximum stress range cannot be easily determined.

Loading scenario	Load step 1	Load step 2	Comment
Scenario 1 – uni-axial loading			Stress range = $\sigma_{max} - \sigma_{min}$ Stress amplitude = $(\sigma_{max} - \sigma_{min})/2$
Scenario 2 – bi-axial loading with unchanging principal axes orientation over load cycle			Stress range = $\tau_1 - \tau_2$ Stress amplitude = $(\tau_1 - \tau_2)/2$
Scenario 2 – bi-axial loading with changing principal axes orientation over load cycle			In this scenario, stress range or amplitude cannot be calculated directly

Figure 38 : Several loading scenario examples

Critical plane fatigue analysis is performed in case of non-proportionally varying stresses i.e., when principal stress directions change over the load cycle. The plane with maximum stress range and damage must be found using a computer code by incremental approach. Figure 39a shows stress component of a membrane element over the loading cycle Figure 39 b shows an example of proportionally varying stresses. When stresses vary proportionally, the shown constant  $k$  is the varying component and the matrix remains same over the loading cycle. Hence, its eigenvectors do not change – principal stress directions remain same. From Figure 39a, it can be inferred that not all components vary in constant ratio with each other. Hence, critical plane analysis is required.

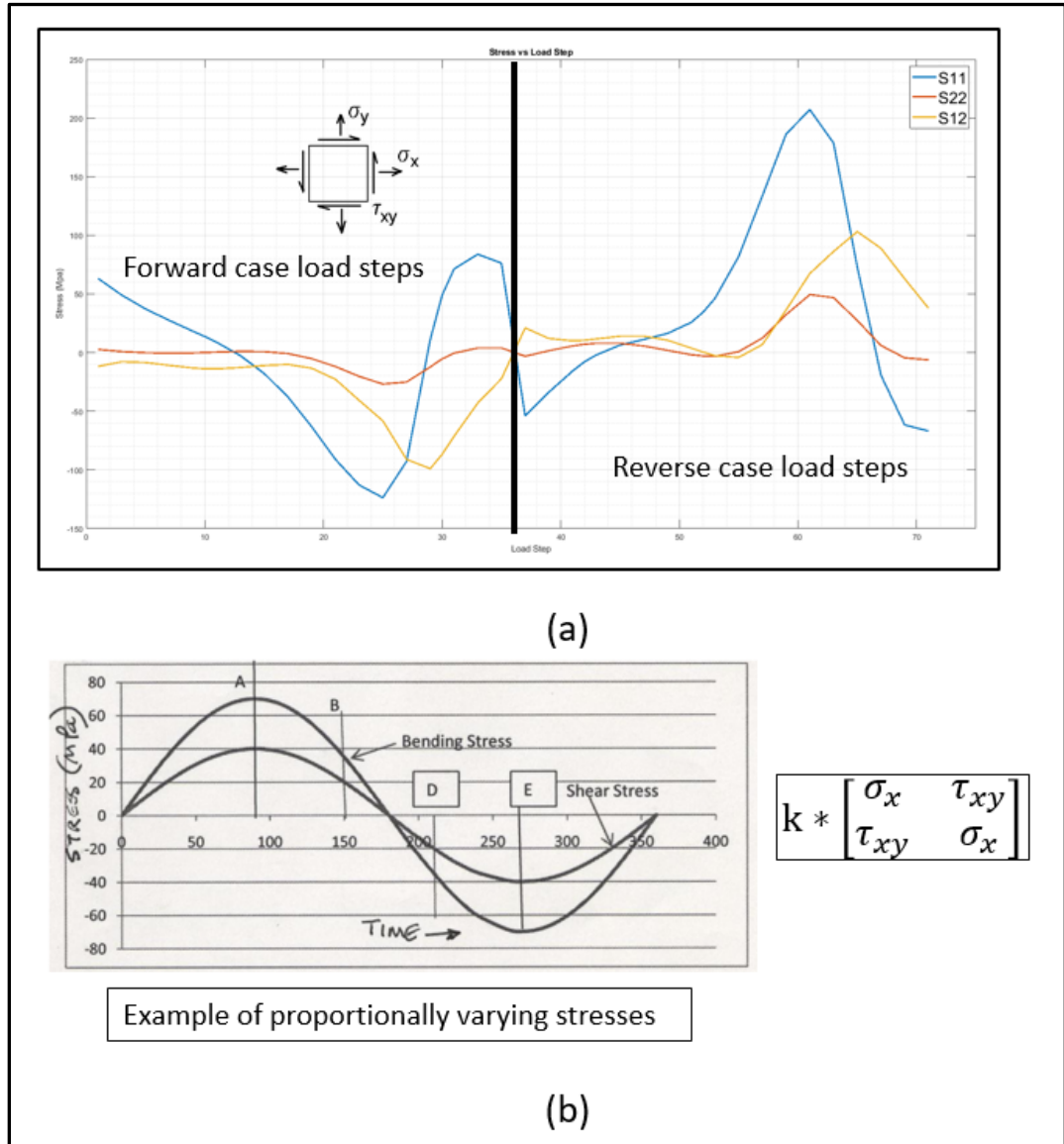


Figure 39 : a) Stress state history of a membrane element b) example of proportionally varying stresses

There are several critical plane models available in literature. In this project, fatigue analysis is done as per a research [6] published in the international journal of fatigue. The method described in this research is chosen as it generalizes the determination of critical plane orientation for all kinds of metals (brittle and ductile).

## 5.2 Ductile Iron S-N curve

The S-N curve of ductile iron is obtained from [7]. Figure 40 shows the digitized curve and fitted equation.

$$f_{Nf} = -10.69 \ln N + 368.75$$

Where  $f_{Nf}$  is the finite life. The blue curve represents the finite life and the orange curve represents infinite life.

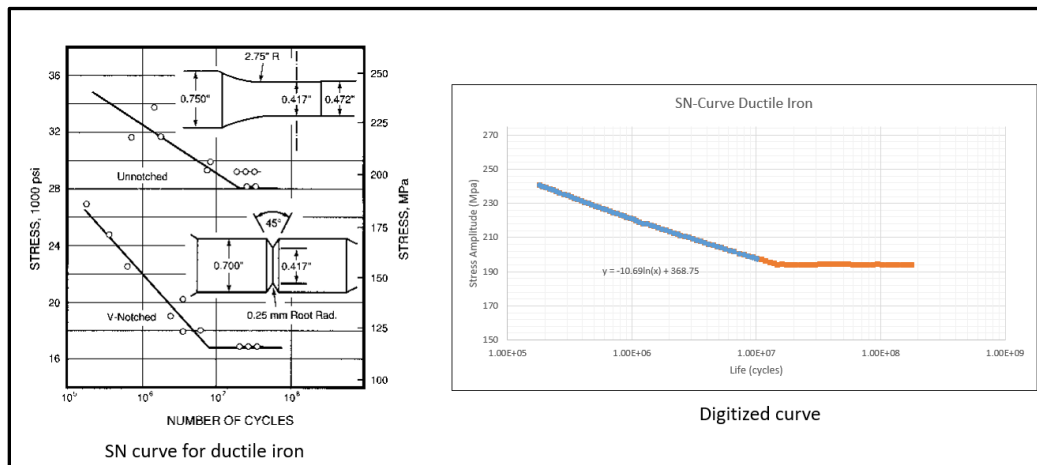


Figure 40 : Ductile iron S-N Curve [7]

## 5.3 Fatigue life prediction method

This section describes the method for finding fatigue fracture plane, critical plane, fatigue damage and fatigue life as detailed in [6].

The following definitions are critical to understanding the methodology.

**Fatigue Fracture Plane (FFP)** - Plane experiencing the maximum normal stress amplitude.

**Critical Plane** – Plane on which fatigue damage is calculated.

One of the major assumptions in this analysis is that the normal of the critical plane lies in the plane of the membrane element. Another assumption is that the given loads from AAM

are scaled by a factor of 2. In fatigue analysis, unscaled loads are to be used. Hence, using linear assumption (stress proportional to load), stresses are factored by a value of 0.5.

Once fatigue fracture plane is determined based on the stress history of the membrane element, critical plane is at an angle  $\alpha$  and is determined by the following relation [6].

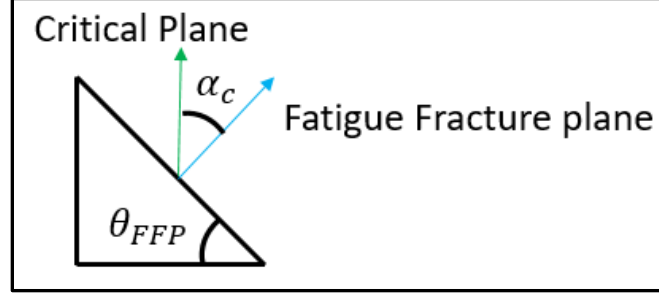


Figure 41: Fatigue fracture and critical plane normals

$$\cos 2\alpha = \frac{-2 + \sqrt{4 - 4\left(\frac{1}{s^2} - 3\right)\left(5 - \frac{1}{s^2} - 4s^2\right)}}{2\left(5 - \frac{1}{s^2} - 4s^2\right)}$$

Where  $s = \frac{t_{-1}}{f_{-1}}$ .  $t_{-1}$  and  $f_{-1}$  are fully reversed fatigue limits of the material in pure shear and pure tension cases respectively. In this analysis it is assumed that  $s = \frac{1}{\sqrt{3}}$ . It's done so because typical value of  $s$  for brittle metals is greater than  $\frac{1}{\sqrt{3}}$  [6], and it means that the least possible shear fatigue limit ( $t_{-1}$ ) is used. This results in a conservative analysis

the assumed value results in a conservative analysis.

The proposed damage model is a nonlinear combination of normal and shear stress amplitudes as shown in the following equation.

$$\sqrt{\left[\frac{\sigma_{a,c} \left(1 + \eta \frac{\sigma_{m,c}}{f_{-1}}\right)}{f_{-1}}\right]^2 + \left(\frac{\tau_{a,c}}{t_{-1}}\right)^2} = \beta$$

$$\beta = \sqrt{\cos^2 2\alpha s^2 + \sin^2 2\alpha}$$

$$\eta = \frac{3}{4} + \frac{1}{4} \left(\frac{\sqrt{3} - \frac{f_{-1}}{t_{-1}}}{\sqrt{3} - 1}\right)$$

Where  $\beta$  is the critical damage value,  $\sigma_{a,c}$  is the normal stress amplitude on the critical plane,  $\tau_{a,c}$  is the shear stress amplitude on the critical plane,  $\sigma_{m,c}$  is the mean stress on the critical plane and  $\eta$  is the mean stress correction factor. This means that when the nonlinear combination of stress amplitudes exceed  $\beta$ , failure occurs.

Once damage is computed for an element, fatigue life can be calculated by solving for  $f_{Nf}$  in the following Finite Life Equation. This equation was solved numerically using MATLAB. It is also assumed that ratio of finite life fatigue strengths,  $\frac{t_{Nf}}{f_{Nf}} = \frac{1}{\sqrt{3}}$ .

$$\frac{1}{\beta} \sqrt{\left[ \frac{\sigma_{a,c} \left( 1 + \eta_F \frac{\sigma_{m,c}}{f_{Nf}} \right)}{f_{Nf}} \right]^2 + \left( \frac{f_{Nf}}{t_{Nf}} \right)^2 (\tau_{a,c})^2} = f_{Nf}$$

For each surface element stress history is extracted using python scripting in ABAQUS and fatigue life is computed as per the above method. A MATLAB code is developed to perform the computations. Figure 42 shows the flow chart for the algorithm developed.

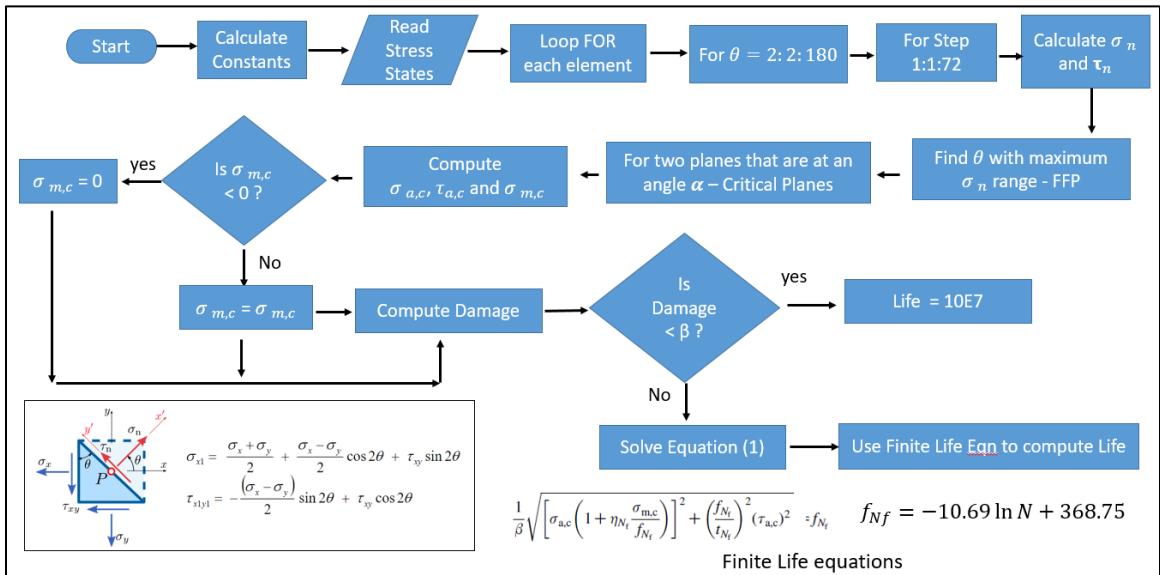


Figure 42 : Fatigue life prediction algorithm

Initially all constants ( $s$ ,  $\alpha$ ,  $\beta$ ,  $f_{-1}$  and  $\eta$ ), are input in the code. The code then loops through each element's stress history. Normal stress range on each plane (parametrized by angle  $\theta$ ) is then determined. The plane experiencing maximum normal stress range is fatigue fracture plane (FFP). Then critical plane is determined (which is at an angle  $\alpha$  to the FFP). The normal and shear stress amplitudes and mean normal stress on the critical plane are used to calculate fatigue damage for that element. If the damage is less than the critical

damage  $\beta$ , the element has infinite life ( $>5,000,000$  cycles), if not finite life equations are numerically solved in MATLAB to obtain fatigue life.

## 5.4 Results

Once fatigue damage and life are computed for each element, it is necessary to view the results at all locations to find potential crack initiation sites. A python script is developed that reads the computed values from MATLAB and creates a custom plot in ABAQUS. Figure 43 shows the fatigue damage contour plots. The contour is capped at the critical damage value of 1 ( $\beta = 1$  for  $s = \frac{1}{\sqrt{3}}$ ). So, the areas where damage exceeds the value 1 are shown in grey. These grey areas have finite life. Figure 44 shows the fatigue life plots. In this figure, contour is reversed, and grey regions have infinite life. All regions which have finite life ( $< 5,000,000$  cycles) are marked with rainbow contour.

Although high cycle fatigue analysis indicates failure regions, because of higher strains (that would occur due to plasticity), stress life method cannot be used to accurately determine life. Strain life method using elastic-plastic material properties should be used to determine fatigue life accurately at these locations. However, it can be said that the regions with finite life or with damage greater than 1 are susceptible to fatigue failure.

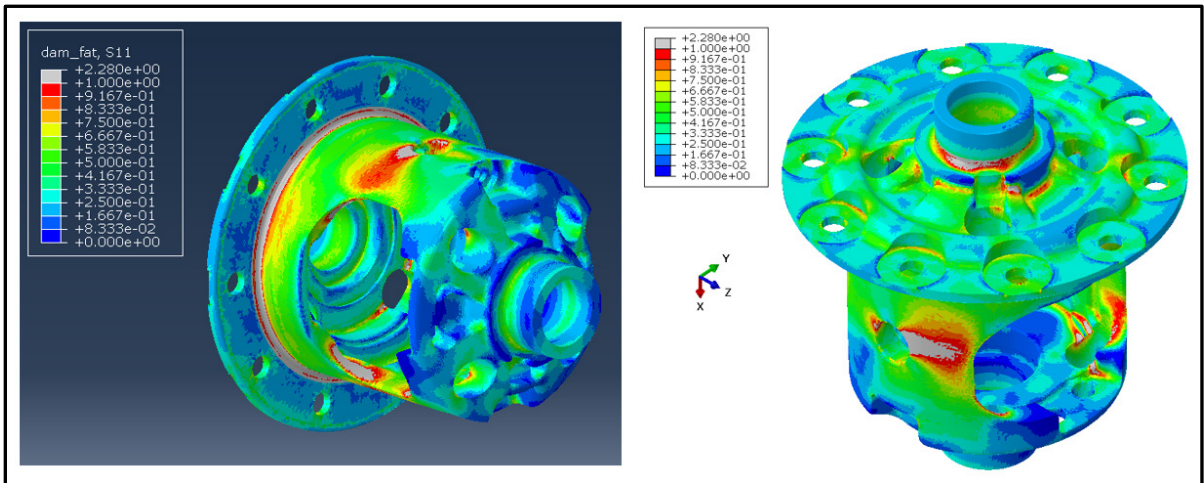


Figure 43: Fatigue damage plot

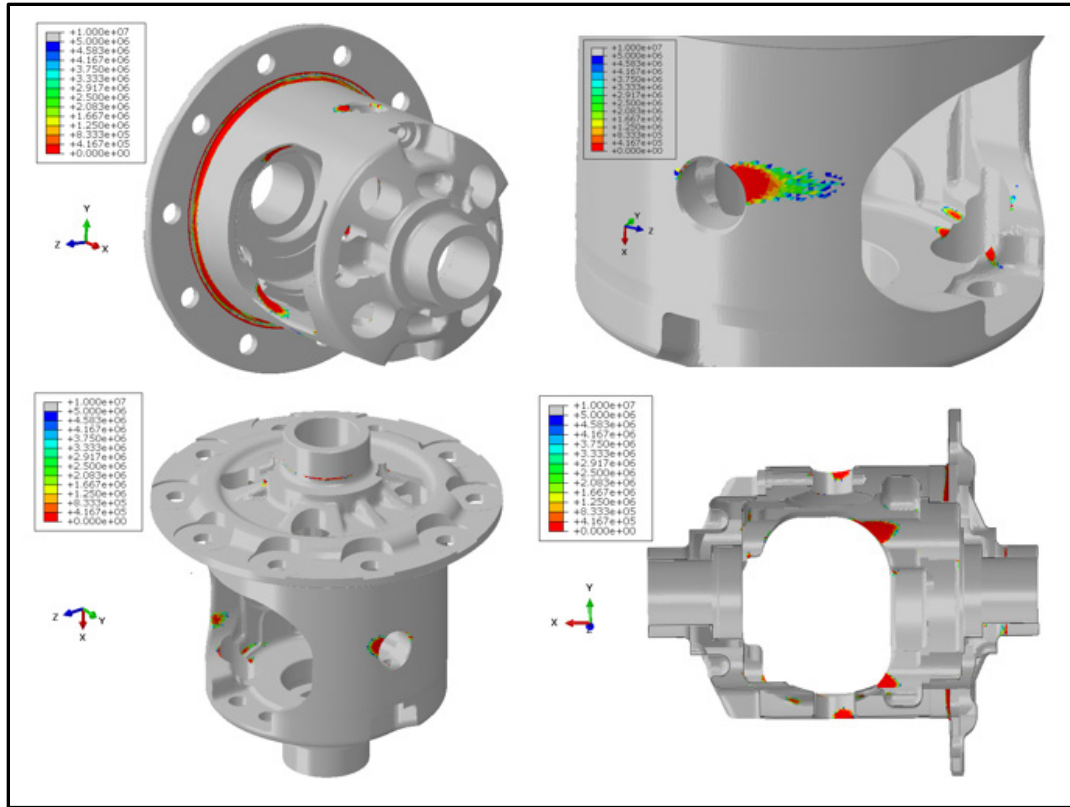


Figure 44 : Fatigue life plots

## 5.5 Conclusions and Future work

The weight of the differential case is reduced by 18.5 % with justifiable violations of the design criteria. Further weight can be reduced by creating geometry more closed to that obtained through topology optimization. Strain life methods can be explored to obtain accurate damage and life estimates at critical locations.

## 6 Reference List

- [1] <http://www.dupont.com/industries/automotive/articles/lightweighting.html>
- [2] [www.matweb.com/search/datasheet.aspx?matguid=9cbba19c60004f58b8f2925b210abaf3](http://www.matweb.com/search/datasheet.aspx?matguid=9cbba19c60004f58b8f2925b210abaf3)
- [3] ABAQUS CAE User's manual 17.6.1
- [4] Practical Aspects of Structural Optimization, A Study Guide, 2<sup>nd</sup> edition – Optistruct
- [5] [https://en.wikipedia.org/wiki/Topology\\_optimization](https://en.wikipedia.org/wiki/Topology_optimization)
- [6] Multiaxial high-cycle fatigue criterion and life prediction for metals, Yongming Liu, Sankaran Mahadevan, International Journal of Fatigue 27, Jan 2005
- [7] [https://www.ductile.org/didata/Section3/Figures/pfig3\\_25.htm](https://www.ductile.org/didata/Section3/Figures/pfig3_25.htm)
- [8] *AAM Clarification PPT 2018*



## A Appendix

This section contains Python and MATLAB scripts developed for the fatigue life evaluation, and design modification detail of the barrel region.

### A.1 Scripts

Below is the python script that extracts stresses from ABAQUS and writes to a csv file.

```
# Get ABAQUS interface
from abaqus import *
from abaqusConstants import *
from odbAccess import *
from abaqusConstants import *
from odbMaterial import *
from odbSection import *
myOdb = session.openOdb(name='trial-27-itr9-rev.odb',readOnly =
False) # Open the odb
session.viewports['Viewport: 1'].setValues(displayedObject=myOdb)
b = 'Step-'
myInstance = myOdb.rootAssembly.instances['DIFFCASE-1'] # Instance
myElem = myOdb.rootAssembly.instances['DIFFCASE-
1'].elementSets['SET-26'] # Element Set of Surface
Elements
x=21 # Counter
for stepName in myOdb.steps.keys(): # Loop over all Load Steps
    if stepName != 'Initial': # Omit 'Initial' Step
        a=[b,str(x),'.csv']
        c = ''.join(a) # String for filename to write
        file = open(c,'w')
        lastFrame = myOdb.steps[stepName].frames[-1] # Frame
        stressField = lastFrame.fieldOutputs['S'] # Stress Field
        field = stressField.getSubset(region = myElem, position =
INTEGRATION_POINT, elementType = 'M3D3') # Stress field of Surface
Elements
        fieldValues=field.values
        for v in fieldValues:
            ELID = v.elementLabel # Loop over each Surface
            Element
            file.write('%1f \t\t %s \t\t %1f\t\t %s \t\t
%1f\t\t %s \t\t %1f\t\t \n' %(ELID,',',v.data[0],
',',v.data[1],',', v.data[-1])) # Write Stress components
            x=x+1
            file.close()
# Close file
myOdb.close()
# Close Odb
```

The extracted stresses are then processed in MATLAB using the following code. MATLAB also outputs a data file that contains fatigue results used for post-processing

```

%%
clear
clc
%%
s=1/sqrt(3);
f1 = 196.4475575;
t1 = f1*s;
alp = 0.5*acos((-2+sqrt(4-4*((1/(s*s))-3)*(5-(1/(s*s))-4*s*s)))/(2*(5-(1/(s*s))-4*s*s)));
bet = sqrt(s*s*cos(2*alp)*cos(2*alp)+sin(2*alp)*sin(2*alp));
alp_rad = alp*180/pi;
ni=0.05;
inc = ni*alp;

%% read files
c1 = 'Step-';
c3 = '.csv';
e1= csvread('Step-1.csv');
elist = e1(:,1);
nElem = length(elist);
S=zeros(2,2,40,nElem);
for j=1:40
    c2 = string(j);
    fileName = strcat(c1,c2,c3);
    M = csvread(fileName);
    for i =1:nElem
        S(:,:,j,i) = 0.5*[M(i,2) M(i,4);M(i,4) M(i,3)];
    end
end

end
LF = zeros(1,nElem);
th = inc:inc:pi;
lth = length(th);
dmg = zeros(1,nElem);
for k=1:nElem
    for v=1:length(th)
        n = [cos(th(v));sin(th(v))];
        ns = [-sin(th(v));cos(th(v))];
        for j=1:40
            sn(v,j) = dot(S(:,:,j,k)*n,n);
            %st(v,j) = dot(S(:,:,j,k)*ns,ns);
            st(v,j) = -0.5*(S(1,1,j,k)-
S(2,2,j,k))*sin(2*th(v))+S(1,2,j,k)*cos(2*th(v));
        end
        snrange(v) = range(sn(v,:));
    end
end

```

```

end
[maxv, indx] = max(abs(snrangle));
if (indx<=1/ni)
    indx1 = indx+1/ni;
    indx2 = lth + (indx-1/ni);
elseif (indx>lth-1/ni)
    indx1 = indx+1/ni-lth;
    indx2 = indx-1/ni;
else
    indx1 = indx+1/ni;
    indx2 = indx-1/ni;
end
snr1(1,k) = range(sn(indx1,:))*0.5;
snt1(1,k) = range(st(indx1,:))*0.5;
smn1(1,k) = (max(sn(indx1,:))+ min(sn(indx1,:)))*0.5;
snr2(1,k) = range(sn(indx2,:))*0.5;
snt2(1,k) = range(st(indx2,:))*0.5;
smn2(1,k) = (max(sn(indx2,:))+ min(sn(indx2,:)))*0.5;
if (smn1(1,k)<0)
    smn1(1,k) = 0;
end
if (smn2(1,k)<0)
    smn2(1,k) = 0;
end
dmg1(1,k) =
sqrt(((snr1(1,k)*(1+smn1(1,k)*0.75/f1))/f1)^2+(snt1(1,k)/t1)^2);
dmg2(1,k) =
sqrt(((snr2(1,k)*(1+smn2(1,k)*0.75/f1))/f1)^2+(snt2(1,k)/t1)^2);
dmg(1,k) = max(dmg1(1,k),dmg2(1,k));
if dmg(1,k)<1
    LF(1,k) = 10^7;
else
    syms fnf1
    syms fnf2
    eqn1 = (1/bet)*sqrt((snr1(1,k)*(1+0.75*smn1(1,k)/fnf1))^2 +
(1/s)*(1/s)*snt1(1,k)*snt1(1,k)) - fnf1 == 0;
    eqn2 = (1/bet)*sqrt((snr2(1,k)*(1+0.75*smn2(1,k)/fnf2))^2 +
(1/s)*(1/s)*snt2(1,k)*snt2(1,k)) - fnf2 == 0;
    F1 = vpasolve(eqn1,fnf1,[1,1250]);
    F2 = vpasolve(eqn2,fnf2,[1,1250]);
    LF(1,k) = exp((368.75-max(double(F1),double(F2)))/10.961);
end
end

zer = zeros(1,nElem);
DMG = transpose([transpose(elist);dmg;LF;zer;zer]);
dlmwrite('dmglist.txt',DMG,'precision',8)

```

For the visualization of fatigue life and damage, another python script is developed which reads the MATLAB output and creates custom plots shown in Figure 43 and Figure 44, in ABAQUS. This code is shown below.

```

from abaqus import *
from abaqusConstants import *
from odbAccess import *
from abaqusConstants import *
from odbMaterial import *
from odbSection import *
import numpy as np # Import Numpy
myOdb = session.openOdb(name='trial-27-itr9-fwd.odb',readOnly =
False) # Open the odb
session.viewports['Viewport: 1'].setValues(displayedObject=myOdb)

impData = np.genfromtxt('dmglst.txt', delimiter = ',')
# Read Damage File
elementList = np.ascontiguousarray(impData[:,0], dtype=np.int32)
# Get element List
damageValues = np.ascontiguousarray(impData[:,1:3],
dtype=np.float32)
myInstance = myOdb.rootAssembly.instances['DIFFCASE-1'] # Instance
stepNew = myOdb.steps['Step-1'] # Step
frame1 = stepNew.frames[-1] # Frame
sField = frame1.FieldOutput(name='dam_fat',description='Fat_Dam',
type=TENSOR_3D_PLANAR, componentLabels=('S11', 'S22', 'S33','S12'),
validInvariants=(MISES,)) # Create Field
sField.addData(position=INTEGRATION_POINT,
instance=myInstance,labels = elementList, data=damageValues) # Add
values to the field
stepNew.setDefaultField(sField)
myOdb.close()
myOdb = session.openOdb(name='trial-27-itr9-fwd.odb',readOnly =
False) # Open the odb
session.viewports['Viewport: 1'].setValues(displayedObject=myOdb)

```

## A.2 Barrel region modifications

It is mentioned in section 3.3.1 that barrel region is modified manually. The modifications done in this region are shown below.

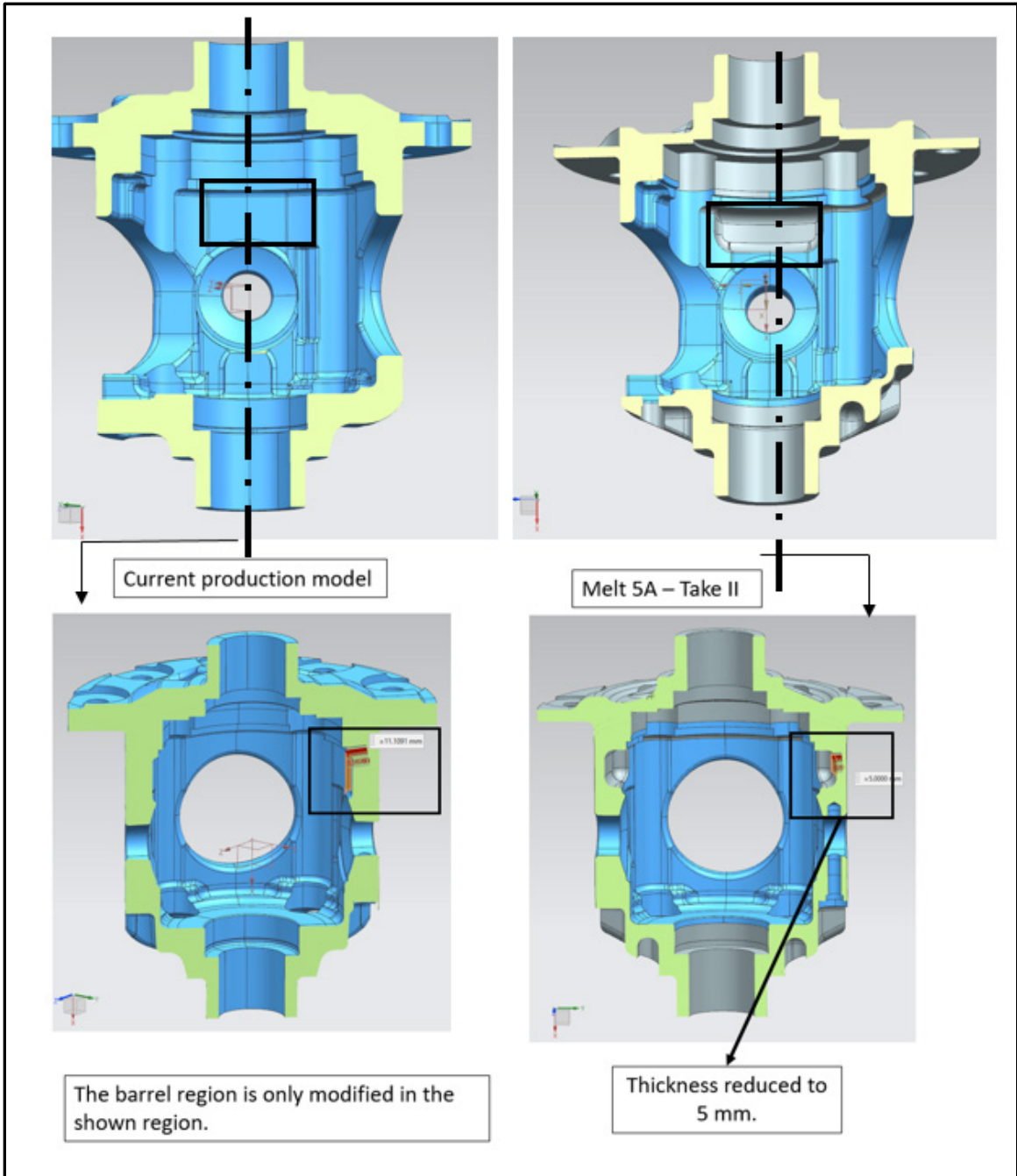


Figure 45: Barrel region material removal